105, Rev. D
Atmospheric and Environmental Effects
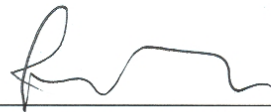
Released September 15, 2009

Prepared by:

Approved by:

S.D.Slobin 9-10-2009

Stephen Slobin   Date
Antenna System Engineer

Timothy T. Pham   Date
DSN Chief System Engineer

Released by:

Signature on File at DSN Library   9/15/2009
DSN Document Release   Date

Change Log

Rev	Issue Date	Affected Paragraphs	Change Summary
Initial	11/30/2000	All	All
A	12/15/2002	All	Provides monthly weather statistics for all stations and frequency bands
B	5/26/2006	2.1, 2.4	Revised weather models, provides new methods for calculating system operating noise temperature and planetary noise effects
C	8/1/2009	Various	Revised weather models and added models for 26 GHz. Removed references to the 26-m subnet which has been decommissioned
D	9/15/2009	Page 18	Corrected the order and labels for Equations (10) and (11)

Note to Readers

There are two sets of document histories in the 810-005 document that are reflected in the header at the top of the page. First, the overall document is periodically released as a revision when major changes affect a majority of the modules. For example, this document is part of Revision E. Second, the individual modules also change, starting as the initial issue that has no revision letter. When a module is changed, a change letter is appended to the module number on the second line of the header and a summary of the changes is entered in the module's change log.

Contents

Illustrations

Illustrations (Continued)

Tables

Tables (Continued)

1 Introduction

1.1 Purpose

This module provides sufficient information concerning atmospheric, environmental, and extraterrestrial effects to enable a flight project to design a telecommunications link at the L-, S-, X-, K-, and Ka-band frequencies used by the DSN.

1.2 Scope

Statistics of atmospheric attenuation and noise temperature at each tracking antenna site are presented for those microwave frequencies used by the DSN. In this module, the values of attenuation and noise temperature increase are given relative to a no-atmosphere (vacuum) condition thus this presentation is compatible for use with the vacuum gain and antenna-microwave noise temperature presentations of antenna performance given in modules 101 for 70-m antennas, 103 for 34-m high-efficiency (HEF) antennas, and 104 for 34-m beam-waveguide (BWG) antennas and the 34-m high-speed beam waveguide (HSB) antenna.

Statistics of wind speed at Goldstone are given. These are used both to determine the statistics of antenna gain reduction due to wind loading and also to ascertain the percentage of time an antenna will be unusable due to excessive wind speed.

Extraterrestrial effects are primarily the increased system noise temperature due to hot body noise from the Sun, Moon, planets, and galactic radio sources. These effects are significant only when the antenna beam is in the vicinity of these noise sources during tracking of spacecraft.

Charged-particle effects are given in module 106, Solar Corona and Solar Wind Effects.

2 General Information

2.1 Atmospheric Attenuation and Noise Temperature

The principal weather-related effects on telecommunications link performance are the atmospheric attenuation and noise temperature resulting from oxygen, water vapor, clouds, and rain. The two effects are related and higher atmospheric attenuation produces a higher noise contribution. Also, atmospheric effects generally increase with increasing frequency, except in the vicinity of the water vapor line at 22.235 GHz (20-25 GHz), and the oxygen band from about 55-65 GHz. K- and Ka-band effects are larger than X-band effects, which in turn are larger than S-band and L-band effects.

In the 810-005 antenna performance modules (modules 101, 103, and 104), *effective antenna gain* (vacuum gain minus atmospheric attenuation) is presented in the figures for various atmospheric attenuation values. Strictly speaking, the gain of an antenna is not a function of atmospheric attenuation; however for stand-alone use, the effective gain, including atmospheric loss, is a useful concept, and the equations for gain in the appendices of those modules include a term for atmospheric attenuation. Similarly, the *antenna-microwave noise temperature, T_{AMW}* (due to spillover, LNA contribution, waveguide loss, etc.), is also not a function of atmosphere. However, the operating system noise temperature as presented in the appendices of the antenna performance modules includes a term for sky noise, which is a combination of atmospheric noise and effective cosmic microwave background noise. Thus the operating system noise temperature is a combination of T_{AMW} and T_{SKY}.

Design control tables (DCTs) used for telecommunications link design typically carry separate entries for atmospheric attenuation of the received or transmitted signal and the atmospheric noise contribution as a function of elevation angle and weather condition. It is important in those DCTs that the antenna gain and antenna-microwave noise temperature values reflect the vacuum performance of the antenna by itself, so as to prevent double-bookkeeping of the atmospheric attenuation and noise temperature contributions.

Four atmospheric models are presented here. The first covers L-band (1.7 GHz) and S-band (2.3 GHz). The second and third cover X-band (8.4 GHz) and Ka-band (32.0 GHz).

The fourth, which is presented in a slightly different format in the tables, covers K-band (25.5 GHz to 27.0 GHz).   Atmospheric noise temperature and attenuation statistics are provided in the form of cumulative distributions (CDs) for each effect. For example, a cumulative distribution of 0.90 ("90% weather") means that 90% of the time a particular weather effect (noise temperature or attenuation) is less than or equal to a given value. Conversely, that particular effect is exceeded 10% of the time. Qualitatively, the weather conditions associated with selected cumulative distributions are described as follows:

CD	=	0.00	clear dry, lowest weather effect
CD	=	0.25	average clear weather
CD	=	0.50	clear humid, or very light clouds
CD	=	0.90	very cloudy, no rain
CD	>	0.95	very cloudy, with rain

By their very natures, clouds and rain are poorly modeled, and the water vapor radiometer data used here are sparse for the larger rain-related weather effects, which are exceeded only 5% of the time.

The Ka-band model presented here is based on actual water vapor radiometer zenith noise temperature measurements made at 31.4 GHz at all three DSN sites (Goldstone, Canberra, and Madrid). These models contain 143 months of Goldstone data covering the period October 1993 through January 2009, 112 months of Canberra data covering the period June 1999 through January 2009, and 189 months of Madrid data covering the period September 1990 through January 2009. There were missing months of data from each station. Note also that different numbers of months of data went into the model for each of the separate months (for example, there may have been 12 Februaries, but only 10 Marches). It is felt that because of the large amount of Madrid data (more than 15 years), the results will fairly accurately represent true long-term statistics. The 12 years of Goldstone data will also give a moderately accurate long-term model. The 9 years of Canberra data will probably give a reasonably accurate long-term model, and future updates of the Canberra model may show relatively large changes in the distributions, particularly at high CD levels (greater than 0.95). Cumulative distributions at 31.4 GHz for each of the 12 months were calculated, then increased by a small amount (0.3 – 3 K, a function of frequency and noise temperature) to create a model for 32 GHz. Year-average models for each station and frequency were generated from the aggregate statistics for all the data.

L/S-band and X-band attenuation statistics were created from the Ka-band (32 GHz) statistics by subtracting out the 0% CD baseline (calculated for nominal temperatures and pressures, with 0% relative humidity), frequency-squaring to the appropriate frequency (for example, $[8.42/32]^2$) and then adding in the 0% CD baseline at the new frequency. Note that the 0% CD baselines for the DSN sites differ because of different heights above sea level. Noise temperature statistics were then derived from the frequency-modeled attenuation statistics.

Noise temperature statistics for zenith were created from the atmospheric attenuation statistics by methods given in Sections 2.1.1 and 2.1.3 below. The year-average noise temperature statistics were calculated from the year-average attenuation values.

For K-band statistics, a somewhat different method was used, rather than the frequency-squared technique described above. It was necessary to do this because atmosphere effects in the 26 GHz region, are starting to be on the high side of the 22 GHz water vapor line, where attenuation and noise temperature values are *increasing* with decreasing frequency. For this reason, the frequency-squaring technique would give inaccurate results. A series of "humid" and "wet" (liquid water cloud) atmosphere models was postulated, that would give the existing Ka-band noise temperature values for each CD value and each station. Then, using these atmospheres, the attenuation and noise temperature were calculated for 25.5, 26.0, 26.5, and 27.0 GHz for the range of CD values at each frequency. The technique and results are described more completely in JPL Publication 09–14 (*Atmosphere Attenuation and Noise Temperature Models at DSN Antenna Locations for 1–45 GHz*, by Anil Kantak and Stephen Slobin, March 2009).

It should be noted that although the noise temperature statistics are the best qualitative measures for comparison of different locations and different frequencies, especially when dealing with low-noise systems (where the atmospheric noise is a large part of the total system noise temperature), the basic data base for the calculation of atmospheric effects is actually the attenuation statistics. Given a station location, frequency, and CD of interest, the attenuation data base value is extracted, modeled to the elevation angle of interest (Section 2.1.2), and then the appropriate atmospheric noise temperature is calculated (Section 2.1.3). Monthly, year-average, and maximum and minimum monthly zenith noise temperature statistics are given in Tables 1 through 9. Similarly, the attenuation statistics are given in Tables 10 through 18. Monthly, maximum, and minimum values are not available for K-band (Tables 19–21).

The atmospheric models thus generated for a particular complex (for example, Goldstone) should be used for all antennas at that complex (for example, DSS-14, DSS-15, DSS-24, etc.), regardless of the small altitude differences among the antennas.

Zenith atmospheric noise temperature statistics for the three DSN sites at L- and S-band are provided in Tables 1 through 3. Tables 4 through 6 provide similar statistics for X-band, and Tables 7 through 9 cover Ka-band. The tables include the maximum and minimum monthly value for each CD level, the year average for that CD level and the average value for each month. These noise temperature statistics should be used only in a qualitative sense to describe the relative levels of atmospheric noise contributions at different locations and cumulative distributions. They should not be used for elevation modeling as this is properly performed using the calculated attenuation at a given elevation angle as a starting point and following the process that is described below.

The use of these statistics depends on the context in which the antenna temperature is stated. When a nominal antenna zenith T_{op} (operating system noise temperature) is stated, it is considered to include the CD = 25% (average clear sky) value for the appropriate frequency and location. However, "vacuum" antenna temperatures, that include the cosmic noise

contribution, are sometimes used to describe the performance of an antenna independent of location. In this case, the operating system noise temperature should be referred to as $T_{op,\,vac}$.

Tables 10 through 18 provide similar presentations for zenith atmospheric attenuation. The tolerances of atmospheric noise temperature and attenuation, as given in Tables 1 through 18, should be considered to be 5% of the stated values at zenith, or 5% of the values calculated for elevation angles other than zenith. (see Section 2.1.5, below).

Tables 19–21 present year-average K-band zenith attenuation and noise temperature values for the three stations over the frequency range 25.5–27.0 GHz.

Figures 1, 2, and 3 show the L/S-band noise temperature statistics for Goldstone, Canberra, and Madrid respectively. Figures 4, 5, and 6 show X-band statistics for the three complexes. Figures 7, 8, and 9 provide the Ka-band statistics. On each figure, the year-average cumulative distribution, the minimum envelope value, and the maximum envelope values are given for all the individual months at each CD value stated in Tables 1 through 9. Curves of zenith attenuation are not given, although using a rule-of-thumb that a medium with 1 dB attenuation at a physical temperature of about 20 C radiates a noise temperature of approximately 60 K, the Ka-band curves can be used to make rough estimates of the zenith attenuation at the various frequencies. This relationship is nearly linear over the range from 0 to 1 dB.

For other frequencies near to the L-, S-, X-, and Ka-bands (within about 5% of the nominal frequencies), the weather-effects models presented here should be used without modification. These models should definitely not be used to infer statistics in the vicinity of the 22.235 GHz water vapor line (20-25 GHz) or the 60 GHz oxygen band, 55-65 GHz.

2.1.1 *Calculation of Mean Atmospheric Physical Temperature*

The mean physical temperature of the atmosphere is modeled to be a function of the cumulative distribution of weather effects. This reflects the assumption that those effects that are of larger value (for example, high noise temperature) occur closer to the surface (for example, rain, low moist clouds) and hence are at a higher average physical temperature than those that have a lesser effect (a clear sky with low humidity). The mean atmospheric physical temperature is modeled as

$$T_p = 255 + 25 \times CD \ , \ \text{K} \tag{1}$$

where

CD = cumulative distribution of weather effect ($0.0 \le \text{CD} \le 0.99$).

Note that the maximum value of T_p thus becomes nearly 280 K, or about 7 C.

2.1.2 *Elevation Angle Modeling*

Only the attenuation should be modeled as a function of elevation angle. The atmospheric noise temperature contribution at any elevation angle can be calculated from the modeled attenuation at that elevation angle. Elevation angle modeling can be performed using

either a flat-Earth or a round-Earth model. A flat-Earth model is used here, wherein the attenuation increases with decreasing elevation angle:

$$A(\theta) = A_{zen} \times AM = \frac{A_{zen}}{\sin(\theta)}, \text{ dB} \tag{2}$$

where

θ = elevation angle of antenna beam

A_{zen} = zenith atmospheric attenuation (dB), as given Tables 10 through 18 of this module

AM = number of air masses $\left(\dfrac{1}{\sin(\theta)} = 1.0 \text{ at zenith} \right)$

The flat-Earth approximation produces a slightly higher attenuation then would be obtained with a round-Earth model for low elevation angles but is valid to within 1% to 3% at a 6-deg elevation angle, depending on the frequency and the amount of water vapor in the atmosphere. Note that in a telecom link design tool, if the atmosphere attenuation is carried as a separate line item, it should NOT also be included in the "effective" antenna gain (antenna gain minus atmosphere attenuation).

2.1.3   *Calculation of Noise Temperature From Attenuation*

An attenuating atmosphere creates a noise temperature contribution to ground antenna system temperature. The atmospheric noise temperature at any elevation angle (θ) is calculated from the attenuation by

$$T_{atm}(\theta) = T_p \left[1 - \frac{1}{L(\theta)} \right], \text{ K} \tag{3}$$

where

T_p = mean physical temperature of atmosphere (K), calculated above

$L(\theta)$ = loss factor of atmosphere = $10^{\left[\frac{A(\theta)}{10} \right]}$

$A(\theta)$ = atmospheric attenuation at any elevation angle (dB), calculated above

Note that typical values of *L* range from about 1.01 to 2.0 (*A* = 0.04 dB to 3 dB)

11

2.1.4 *Cosmic Background Adjustment*

The noise temperature contribution of the cosmic microwave background is reduced by atmospheric attenuation. For all DSN frequencies the cosmic background noise temperature before atmospheric attenuation is

$$T_{CMB} = 2.725 \text{ K} \tag{4}$$

With atmosphere attenuation, the effective cosmic background becomes

$$T'_{CMB}(\theta) = \frac{T_{CMB}}{L(\theta)}, \text{ K} \tag{5}$$

where

T_{CMB} = cosmic microwave background noise (K) without atmosphere

$L(\theta)$ = loss factor of atmosphere at the elevation angle of interest, as calculated from Section 2.1.3.

The antenna modules (101 Rev. B, 103 Rev. B, and 104 Rev. D) present a system operating noise temperature, T_{op}, consisting of two parts – an *antenna-microwave* component, T_{AMW}, for the contribution of the antenna and microwave hardware, and a *sky* component, T_{sky}, which consists of the atmosphere noise plus the cosmic microwave background noise, attenuated by the atmosphere loss. The T_1 and T_2 coefficients associated with T_{AMW}, are given in the Appendices of the antenna modules, and the appropriate equation to use is also be stated. Thus, for these modules, the system operating noise temperature with atmosphere and with attenuated cosmic contribution becomes

$$T_{op}(\theta) = T_{AMW} + T_{sky} = \left[T_1 + T_2 e^{-a\theta}\right] + \left[T_{atm}(\theta) + T'_{CMB}(\theta)\right] \tag{6}$$

where

T_1, T_2 and a are coefficients from the telecommunications interface modules

T_{atm} is the atmosphere noise term, given above

T'_{CMB} is the attenuated cosmic noise, given above

2.1.5 *Example of Use of Attenuation Statistics to Calculate Atmospheric Noise Temperature, $T_{atm}(CD,\ \theta)$, and $T_{op}(CD,\ \theta)$*

The following example will show a typical calculation of atmospheric attenuation and noise temperature for a particular situation. The parameters for the example are

DSS-43, Canberra

Ka-band (32 GHz)

90% year-average weather (CD = 0.90)

20-deg elevation angle (2.924 air masses)

From Table 17, the year-average zenith attenuation for CD = 0.90 is given as

$$A_{zen} = 0.403 \text{ dB}$$

The attenuation at 20-deg elevation is

$$A\left(90\%, 20^\circ\right) = \frac{0.403}{\sin\left(20\right)} = 1.178 \text{ dB}$$

Note that in a telecom link design tool, if the atmosphere attenuation is carried as a separate line item, it should NOT also be included in the *effective antenna gain* (antenna gain minus atmosphere attenuation).

The loss factor *L* at 20-deg elevation is

$$L\left(90\%, 20^\circ\right) = 10^{1.178/10} = 1.312$$

The atmospheric mean physical temperature is

$$T_p = 255 + 25 \times 0.90 = 277.5 \text{ K}$$

The atmospheric noise temperature at 20-deg elevation is

$$T_{atm}\left(90\%, 20^\circ\right) = 277.5\left[1 - \frac{1}{1.312}\right] = 65.991 \text{ K}$$

The effective cosmic background temperature at 20-deg elevation is

$$T'_{CMB} = \frac{2.725}{1.312} = 2.077 \text{ K}$$

The operating system noise temperature at 20-deg elevation is

$$T_{op}\left(90\%, 20^\circ\right) = T_{AMW}\left(20^\circ\right) + 65.991 + 2.077 = T_{AMW}\left(20^\circ\right) + 68.068 \text{ K}$$

where

$T_{AMW}(\theta)$ is obtained from revisions of the telecommunications interface modules published after May, 2006.

The "old" (before May, 2006) formulation in the telecommunications interface modules includes the cosmic microwave background in $T_{op,vac}(\theta)$, and the operating system noise temperature at any elevation angle for any weather condition is given by

$$T_{op}(CD,\theta) = T_{op,vac}(\theta) + T_{atm}(CD,\theta), \text{ K} \tag{7}$$

where

$T_{op,vac}(\theta)$ is obtained from revisions of the telecommunications interface modules published before May, 2006.

For this example using the old formulation, the operating system noise temperature at 20-deg elevation is

$$T_{op}\left(90\%, 20°\right) = T_{op,vac}\left(20°\right) + T_{atm}\left(90\%, 20°\right) = T_{op,vac}\left(20°\right) + 65.991 \text{ K}$$

2.1.6 Best/Worst Month Ranges of Atmospheric Noise Temperature and Attenuation

The absolute accuracy of the 31.4-GHz water vapor radiometer measurements used to create the noise temperature statistics is thought to be a few tenths K to 2 K at zenith. The month-to-month variation of average noise temperature at any CD varies much more than this at all values of cumulative distribution greater than about 10%. A particular month might be the "worst" at the 90% CD level, but merely "moderate" at lower CD levels. An example is a winter month that has a large amount of rain, but when not raining has low humidity and low noise temperature contribution. At this time, there are insufficient data to characterize "best" and "worst" months individually; however, tolerances on the mean statistics as given in Tables 1 through 18 can give the user a feeling of what yearly variations in atmospheric effects may be expected.

Inspection of Tables 1 through 18 and Figures 1 through 9 will show that fictitious "best month" and "worst month" statistics can be generated from the values giving the minimum and maximum envelope values of noise temperature and attenuation, without regard to the variability among the months as a function of CD. At high values of CD, the adverse (maximum envelope) yearly tolerances can be as high as 40% of the year-average value of an effect. It should be noted that adverse tolerances for both noise temperature and attenuation give INCREASES from the values in Tables 1 through 18. An adverse VALUE is a mean PLUS the adverse tolerance. For mission planning purposes, with no need to create a model for a specific month, it may be sufficient to use the year-average value at a particular CD, and use the maximum/minimum envelope values to define very conservative (large) adverse/favorable tolerances, with triangular distribution. For specific-month planning purposes, it may be sufficient to use the values given in Tables 1 through 18, with ±5% tolerances (triangular

distribution) as stated above. A very conservative approach (acknowledging that any individual month in the future can be well outside the historical range of available data) would be to use the "maximum" envelope as the model for a possible "bad" month. Note also that for particular months characterized by "bad weather", year-to-year variation of noise temperature and attenuation statistics can be quite large.

2.2 *Rainfall Statistics*

To assist the user in determining which months may have large rainfall-related atmospheric noise temperature and attenuation increases, rainfall data are presented for the three DSN antenna locations. Months with large average rainfall amounts may not necessarily correspond to months with large noise temperature and attenuation values. Comparison with Tables 1 through 18 should be made.

Table 22 presents the monthly and year-average rainfall amounts for the three DSN antenna locations. The Goldstone data (1973–2000) were taken at the administration center, located near the middle of the Goldstone antenna complex. Some antennas may be located as much as 10 miles from this location. The Canberra data (1966–2002) were taken at the Tidbinbilla Nature Reserve, located about 3 miles southwest of the antenna site. The Madrid data (1961–1990) are the averages of the rainfall at two locations: Avila, about 20 miles northwest of the antenna site, and Madrid (Quatro Vientos) about 20 miles east of the antenna site. Although these averages may not exactly reflect the rainfall at the antenna site, the relative monthly amounts are undoubtedly correct.

2.3 *Wind Loading*

The effect of wind loading must be modeled probabilistically, since wind velocity varies randomly over time and space. Figure 10 shows the probability distribution of wind speed for Goldstone. Similar data for the Madrid and Canberra complexes will be supplied when available. The wind load on a particular antenna is dependent on the design of that antenna. Consequently, information about wind-load effect on antenna gain is listed in the appropriate antenna module.

Statistics show that Goldstone is the windiest of the three Deep Space Network antenna complexes. The DSS-14 70-m antenna is *stowed* (pointed vertically) when wind gusts exceed 55 mph (88 km/hr). The frequency of occurrence of this event can be deduced from a relationship between wind gusts and average wind speed. This relationship is found to be: maximum hourly wind speed = 0.62 × strongest gust. Thus, for 55-mph (88 km/hr) gusts, the maximum hourly wind speed is found to be 34 mph (55 km/hr). From Figure 10, it is seen that this speed is exceeded approximately 2 % (175 hours) of the year and 4 % (29 hours) of the worst month. Actual practice has shown that no antenna has been stowed more than about 10 hours per year due to excessive wind-gust occurrences.

2.4 *Hot Body Noise*

2.4.1 *Solar Noise*

The increase in system noise when tracking near the Sun depends on the intensity of solar radiation at the received frequency and on the position of the Sun relative to the antenna gain pattern. The subreflector support structure (typically a quadripod, but a tripod at the DSS-13 BWG antenna) introduces non--uniformities in the sidelobe structure. Increases in noise temperature are typically greater in directions at right angles to the planes established by the subreflector support legs and the center of the reflector surface. Thus, a quadripod-type antenna will have four enhanced regions of noise temperature, and a tripod-type antenna will have six. With an azimuth-elevation (AZ–EL) or X/Y mounted antenna, the plane containing the Sun–Earth–Probe (SEP) angle will rotate through the sidelobes during a tracking pass. This causes the solar noise to fluctuate during a track even if the SEP angle is constant.

A large number of measurements were made at Goldstone from 1987 to 1996 to determine the system noise temperature effects of tracking near the Sun (within about five deg from the center of the solar disk). These measurements were made at S-band on the 26-m antennas and at S-, X-, and Ka-bands on the 34-meter antennas.

Figure 11 shows the 10.7-cm (2800-MHz) solar radio flux during the period of January 2001 through December 2015 covering the end of solar cycle 23 and the beginning of solar cycle 24. The flux is measured in solar flux units (SFU) where one SFU = 1×10^{-22} W/m^2/Hz. Updated solar flux predictions can be found at the National Oceanic and Atmospheric Administration (NOAA) Space Environment Center web site <http://www.sec.noaa.gov/weekly.html> (Solar Cycle Progression and Prediction Plots). Solar flux predictions can be used to model S- and X-band solar noise temperature contributions using the ratio of predicted solar flux to the solar flux that existed at the time the antenna noise temperatures were measured.

The general characteristic of the 11-year cycle of 2800-MHz solar flux is a rapid rise to a peak approximately 4–5 years after the minimum, followed by a 7–6 year gradual decrease. From cycle to cycle, the peak flux can vary by as much as a factor of two. The 10.7-cm flux varied during solar cycle 23 from a minimum of about 70 SFU during 1996 to a maximum of about 225 ± 15 SFU in late 2001 and will return to an expected minimum of about 70 SFU during early 2007.

Figure 12 shows X-band system noise temperature increases as measured at the Goldstone DSS-15 HEF antenna. These measurements show the increased effect for the Sun located (offset) at right angles to the quadripod legs. The quadripod legs are arranged in an "X" configuration, with 90-deg spacing. The measurements were made in November 1987 (near the beginning of the solar cycle) with a measured 2800-MHz flux value of 101 SFU and an 8800-MHz flux value of 259 SFU. The following expression may be used as an upper limit of X-band solar noise contribution at DSS-15 as shown in Figure 12.

$$T_{sun} = 800e^{-2.0\theta}, \text{K} \tag{8}$$

where

θ =   offset angle between center of beam and center of solar disk, deg

Figure 13 shows S-band (2295 MHz) solar noise contribution for a 34-meter diameter antenna. This curve is based on measurements made on a 26-meter diameter antenna, and the angular offset values were modeled by the ratio of antenna beamwidths. The noise temperature measurements were originally made on the Goldstone DSS-16 26-m antenna on December 20, 1989. The reported 2800-MHz solar flux at the time of the experiment was 194 SFU; at 8800 MHz it was 290 SFU. Note that compared to the November 1987 flux (Figure 12), the 2800-MHz flux has nearly doubled, but the 8800-MHz flux has only increased about 12 percent. The S-band solar noise contribution shown in Figure 13 can be modeled as

$$T_{sun} = 1400e^{-1.8\theta}, \text{K} \tag{9}$$

where

θ =   offset angle between center of beam and center of solar disk, deg

This equation undoubtedly underestimates the solar noise contribution at offset angles less than 1 degree by hundreds of K.

Figures 14 and 15 are contour plots of the DSS-12, 34-m HA–DEC total system noise temperature versus declination and cross-declination antenna pointing offsets. DSS-12 has been decommissioned since the measurements were made, but the figures are included because they are representative of the effects of the quadripod on solar noise at other antennas. The quadripod legs are arranged in a "+" configuration with 90-deg spacing, hence the peaks at right angles to the legs.

Figure 14 is a contour plot of total S-band system noise temperature versus declination and cross-declination antenna pointing offsets at DSS-12.The contour interval is 50 K. These measurements were made on January 12, 1990. On this day the reported 2800-MHz solar flux was 173 SFU.

Figure 15 is a contour plot of total X-band system noise temperature versus declination and cross-declination antenna pointing offsets at DSS-12. The contour interval, measurement date, and flux values are identical with those in Figure 14. The reported 8800-MHz solar flux was 272 SFU.

Figures 16 and 17 show the X-band (8.4-GHz) and Ka-band (32-GHz) solar noise contributions at the DSS-13, 34-m research and development beam waveguide antenna as a function of offset angle from the center of the sun. These data were taken during mid-March, 1996, when the 10.7-cm solar flux was about 70 SFU (the minimum at the end of solar cycle 22

and at the beginning of solar cycle 23) and should be considered as representative of what is expected at the operational DSN beam waveguide antennas.

The following expressions give an approximate upper envelope for the noise contributions shown in Figures 16 and 17 as a function of offset angle

$$T_{sun} = \begin{vmatrix} 5000e^{-6.6\theta}, 0.35 < \theta \le 0.75\,\text{deg} \\ 100e^{-1.4\theta}, \theta > 0.75\,\text{deg} \end{vmatrix}, \text{ at X-band.} \tag{10}$$

$$T_{sun} = \begin{vmatrix} 1400e^{-5.1\theta}, 0.35 < \theta \le 0.75\,\text{deg} \\ 86e^{-1.4\theta}, \theta > 0.75\,\text{deg} \end{vmatrix}, \text{ at Ka-band} \tag{11}$$

At offset angles less than 0.35 deg (0.08 deg from the edge of the solar disk), solar noise contributions are likely to be in excess of 300 K at both frequencies. At offsets greater than 4.0 degrees, the solar contribution is negligible.

All noise contribution expressions given above should be compared with values shown in the corresponding figures to assess their validity. Note that these expressions should be considered valid only for the flux values given at the time of measurement. For predictive purposes, Figure 11 may be used to obtain future predicted 2800-MHz solar flux, and the noise contributions at S- and X-band can be modeled as described below.

During the 11-year solar cycle, the S-band flux varies by a factor of 3 (reference Figure 11) while the corresponding X-band flux varies by a factor of 2. For cycle 23, when the S-band range is expected to be from 70 SFU to as much as 210 SFU, the X-band range is predicted to be from about 200 SFU to about 400 SFU. The predicted X-band flux can be derived from the predicted S-band flux by the following expression.

$$\text{FLUX}, X = 200 + \frac{200(\text{FLUX}, S - 70)}{140} \tag{12}$$

For example, in January 2003 the mean S-band flux is predicted to be 125 SFU (from Figure 11). The mean predicted X-band flux would be 264 SFU.

The predicted solar noise contribution can be calculated based on measured noise contributions described above. For example, using the equation provided for Figure 12 (Equation 8) and the predicted X-band solar flux in January of 2002 (264 SFU), the predicted X-band solar noise contribution for a 2-degree offset angle using the 34-m HEF antenna would be

$$T_{sun} = \frac{264}{259} 800e^{-2.0 \times 2.0} = 14.6\,\text{K} \tag{13}$$

At Ka-band, the solar flux varies little over the solar cycle and the relationship between noise temperature increase and offset angle depicted in Figure 17 can be used at all times.

Figure 18 shows examples of measured S-band system noise temperature made with a 64-m antenna tracking Pioneer 8 (November 1968, near the solar maximum) and Helios (April 1975, near the solar minimum). For all practical purposes, these curves may be used to predict S-band performance for the DSN 70-m antennas. The "maximum" and "minimum" curves for each month show the solar "clock angle" effect due to sidelobes at right angles to the quadripod legs.

Figure 19 shows a theoretical curve of X-band 70-m antenna noise temperature as a function of SEP angle. This curve is generated based on an assumed X-band blackbody disk temperature of 23,000 K, representing an "average" value during the solar cycle. An expression giving quiet Sun brightness temperature, T_b (K), as a function of wavelength (mm) has been found to be

$$T_b = 5672\lambda^{0.24517}, \quad K \tag{14}$$

For S-band (2.3 GHz), T_b = 18700 K. For X-band (8.5 GHz) T_b = 13600 K. For Ka-band (32 GHz) T_b = 9750 K. The active Sun may be expected to have an X-band brightness temperature of as much as two to four times as high as the 13600 K calculated above. Other studies give the X-band solar disk temperature minimum, average, and maximum values over the solar cycle as 14,000 K, 22,000 K, and 30,000 K. At Ka-band these values are 7500 K, 10,000 K, and 12,500 K.

2.4.2   *Lunar Noise*

For an antenna pointed near the Moon, a noise temperature determination similar to that made for the Sun should be carried out. The blackbody disk temperature of the Moon is about 240 K at X- and Ka-bands, somewhat lower at S-band (220 K), and its apparent diameter is almost exactly that of the Sun's (approximately 0.5 deg). Figures 12 through 19 may be used for lunar calculations, with the noise temperature values scaled by 240/23000. Figures 13, 14, 15, and 18 include clear-sky system noise temperatures, which must be subtracted out before scaling in order to determine the lunar noise temperature increase. Nevertheless, at offset angles greater than 2 deg, the lunar noise contribution is negligible. For rough calculations using antenna patterns with half-power beamwidths less than about 20% of the lunar diameter (all DSN antennas at X- and Ka-bands and the 70-m antennas at S-band), more than 90% of the antenna power is on the lunar disk when centered on the moon. In this case, the maximum noise temperature seen is roughly

$$T_{moon} = T_b \times 0.90 \times \eta_{ant}, \text{ K} \tag{15}$$

where

T_b = 240 K

η_{ant} = antenna efficiency ≈ 0.70 for most large antennas

Thus, the peak noise contribution from the moon for any DSN antenna except the 34-m BWG antenna at S-band will be approximately 150 K. Measurements on the DSS-13 34-m beam waveguide antenna (S-band half-power beamwidth ≈ 0.25 deg) yield a noise temperature increase due to the moon of about 136 K, which is nearly constant over the lunar monthly cycle. Measurements at new moon yield a noise contribution of 188K at X-band, and 156 K at Ka-band. Peak noise temperatures about 3-4 days after full moon at X-band and Ka-band were in the range of about 190-200 K.

2.4.3   *Planetary Noise*

The increase in system noise temperature when tracking near a planet can be calculated by the formula

$$T_{pl} = \left(\frac{T_k G d^2}{16 R^2} \right) e^{-2.77 \left(\theta / \theta_0 \right)^2}, \text{ K} \tag{16}$$

where

T_k = blackbody disk temperature of the planet, K

d = planet diameter, km

R = distance to planet, km

θ = angular distance from planet center to antenna beam center

θ_0 = antenna half-power beamwidth (full beamwidth at half power)

G = antenna gain ratio $\left[10^{\left(G(\text{dBi})/10 \right)} \right]$ including atmospheric attenuation.

An alternative method for calculating the noise contribution for a planetary disk somewhat smaller than the antenna beamwidth is presented in JPL document D-33697 (*System Noise Temperature Increase from the Sun, Moon, or Planet Blackbody Disk Temperature*, by Anil Kantak and Stephen Slobin, December 1, 2005). Figure 20 shows an excerpt from that document (Figure 8), that indicates the percentage of total antenna power on a planetary disk, for ratios of half-power beamwidth to disk angular diameter in the range 2.0 to 5.0. For other half-power beamwidth/diameter ratios, that document should be consulted.

For a particular case (Venus on February 1, 2006, as seen from the DSS-13 34-m beam waveguide antenna at X-band), the following calculation is made:

planet diameter (d) = 12,104 km

planet disk temperature (T_k) = 634 K at X-band (Table 23)

range from earth (R) = 0.318 AU = 47,572,800 km

disk angular diameter $\left(\tan^{-1}\left[\dfrac{d}{R}\right] \right)$ = 0.0146 degrees

half-power beamwidth (θ_0) = 0.066 degrees

beamwidth/diameter = 4.521

power ratio from Figure 20 = 0.041

antenna efficiency (η) = 0.673 without atmospheric loss at 39 deg. elevation

$\qquad\qquad$ = 0.663 with clear sky atmospheric loss at 39 deg. elevation

The noise temperature calculated for the Figure 20 example is

T_{venus} = 634 × 0.041 × 0.663 = 17.23 K

Using Equation 16 above, the numerical gain of the DSS-13 antenna is first calculated using an efficiency of 0.663 (includes clear sky atmosphere loss),

$$G = \eta\left(\frac{\pi D}{\lambda}\right)^2 = 5{,}966{,}230 \tag{17}$$

where

$\qquad D \quad = \quad$ antenna diameter = 34 m

$\qquad \lambda \quad = \quad$ wavelength = 0.0356 m at 8420 MHz (X-band)

therefore

$$T_{venus} = \left(\frac{634 \times 5{,}966{,}230 \times 12{,}104^2}{16 \times 47{,}572{,}800^2}\right) = 15.30 \text{ K}$$

The measured noise temperature increase from Venus was 16.18 K, so Equation (16) gives an estimate about 5.4% low, and the Figure 20 method gives an estimate about 6.5% high.

Table 23 presents all the parameters needed for calculation of planetary noise contributions. Also given are the maximum values of expected X-band and Ka-band noise contributions for the mean minimum distance from Earth, with the antenna beam pointed at the center of the planet (θ=0). Corresponding S-band noise temperature increases will be approximately 1/13 as large as the X-band increases because of the lower antenna gain (wider beamwidth) at the lower frequency.

In the case of Jupiter, there is a significant and variable non-thermal component of the noise temperature. Thus the effective blackbody disk temperature at S-band appears to be much higher than at X-band. The S-band noise temperature increase will be approximately 1/6 the X-band values for average Jupiter emission; it will be about 1/3 the X-band values for maximum Jupiter emission. Except for Venus and Jupiter at inferior conjunction (minimum distance), the noise contribution from the planets at S-band is negligible.

The expression (Equation 16) for T_{pl} assumes that the angular extent of the radiating source is small compared to the antenna beamwidth. This approximation is adequate at X-band except for Venus near inferior conjunction (apparent diameter = 0.018 deg) using a 70-m antenna at X-band (beamwidth = 0.032 deg). At Ka-band with a 34-m antenna (beamwidth = 0.0174 deg), the approximation is not adequate for Venus near inferior conjunction and may not be adequate for Mars near inferior conjunction (apparent diameter = 0.005 deg). The expression also assumes that the antenna main beam has a Gaussian shape, with circular symmetry. Antenna gains and half-power beamwidths are given in modules 101, 103, and 104.

2.4.4 Galactic Noise

The center of the Milky Way galaxy is located near –30 degrees declination, 17 h 40 min right ascension. It is possible for a spacecraft with a declination of –30 deg to be in the vicinity of the galactic center, and an increase of system noise temperature would then be observed. A declination of –30 degrees is not typically achieved by spacecraft moving in the plane of the ecliptic, but there are some circumstances (for example, a flight out of the ecliptic) where this location may be observed. Galactic noise temperature contributions at frequencies above 10 GHz are typically insignificant. At S-band, looking directly at the galactic center, a noise temperature increase of about 10 K would be observed. A map of the galactic noise distribution can be seen in chapter 8 of the classic reference J. D. Kraus, *Radio Astronomy*, Cygnus-Quasar Books, Powell, Ohio, 1986.
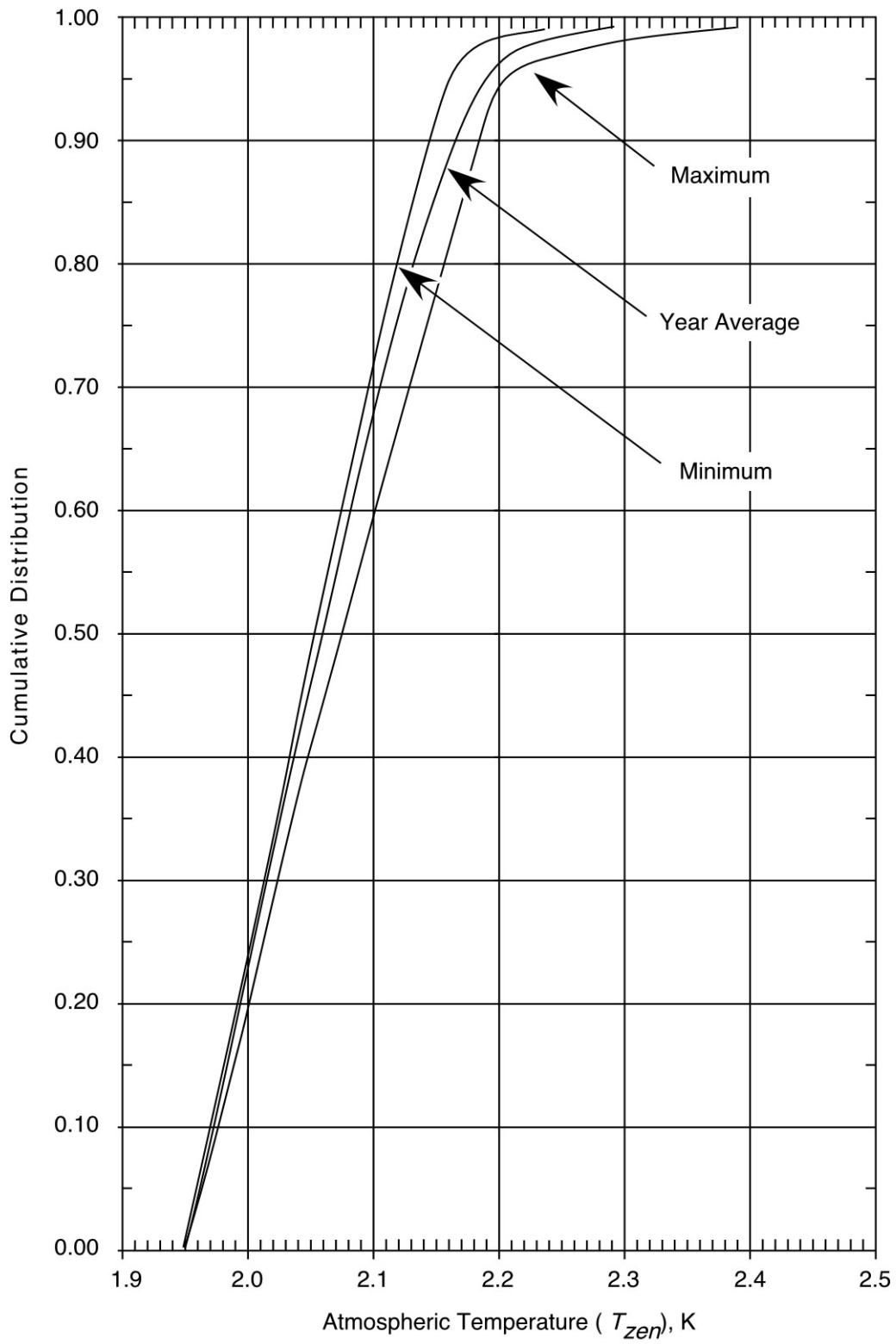
Figure 1. Cumulative Distributions of Zenith Atmospheric Noise Temperature
at L-Band and S-Band, Goldstone DSCC
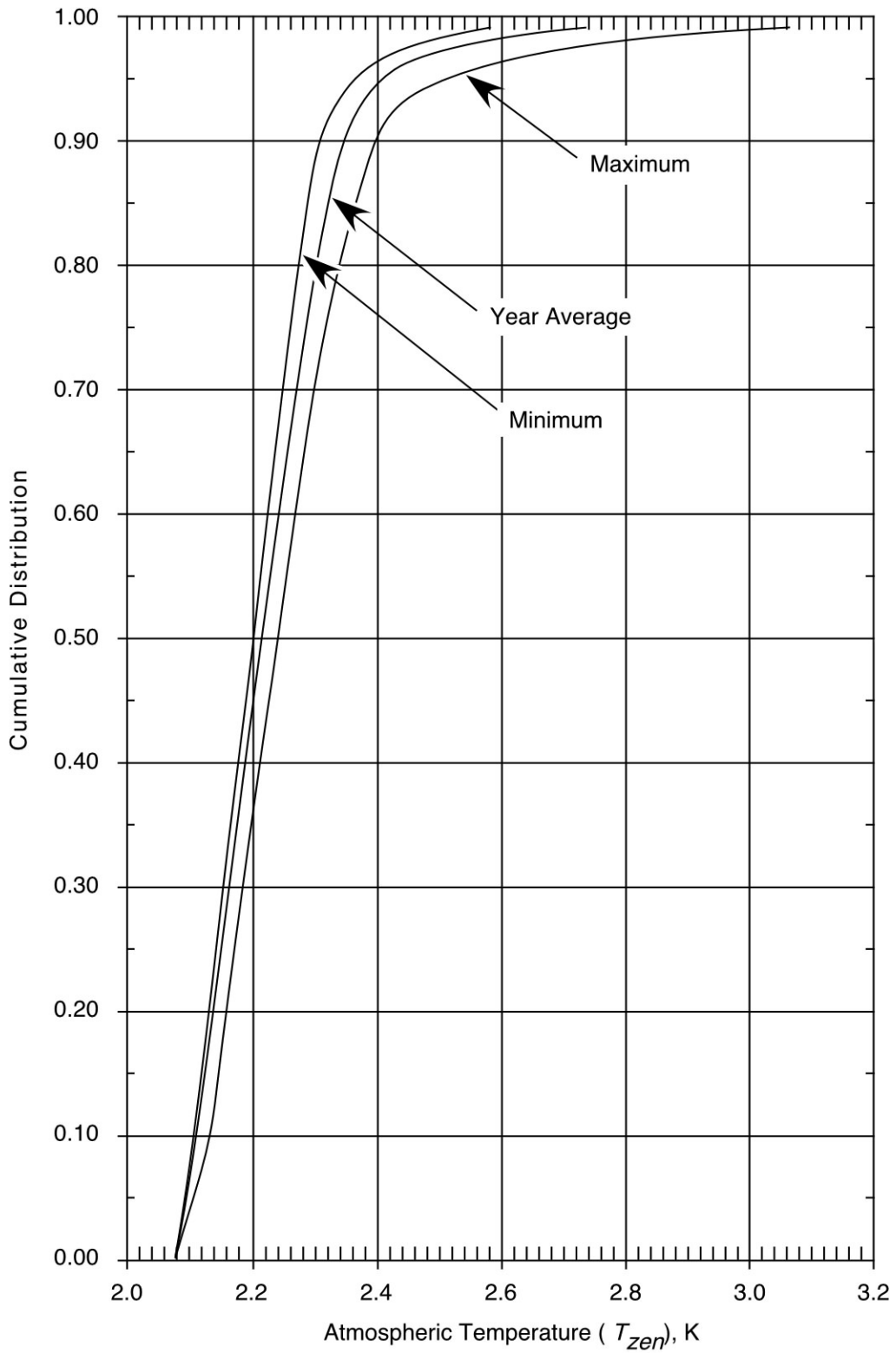
Figure 2. Cumulative Distributions of Zenith Atmospheric Noise Temperature
at L-Band and S-Band, Canberra DSCC
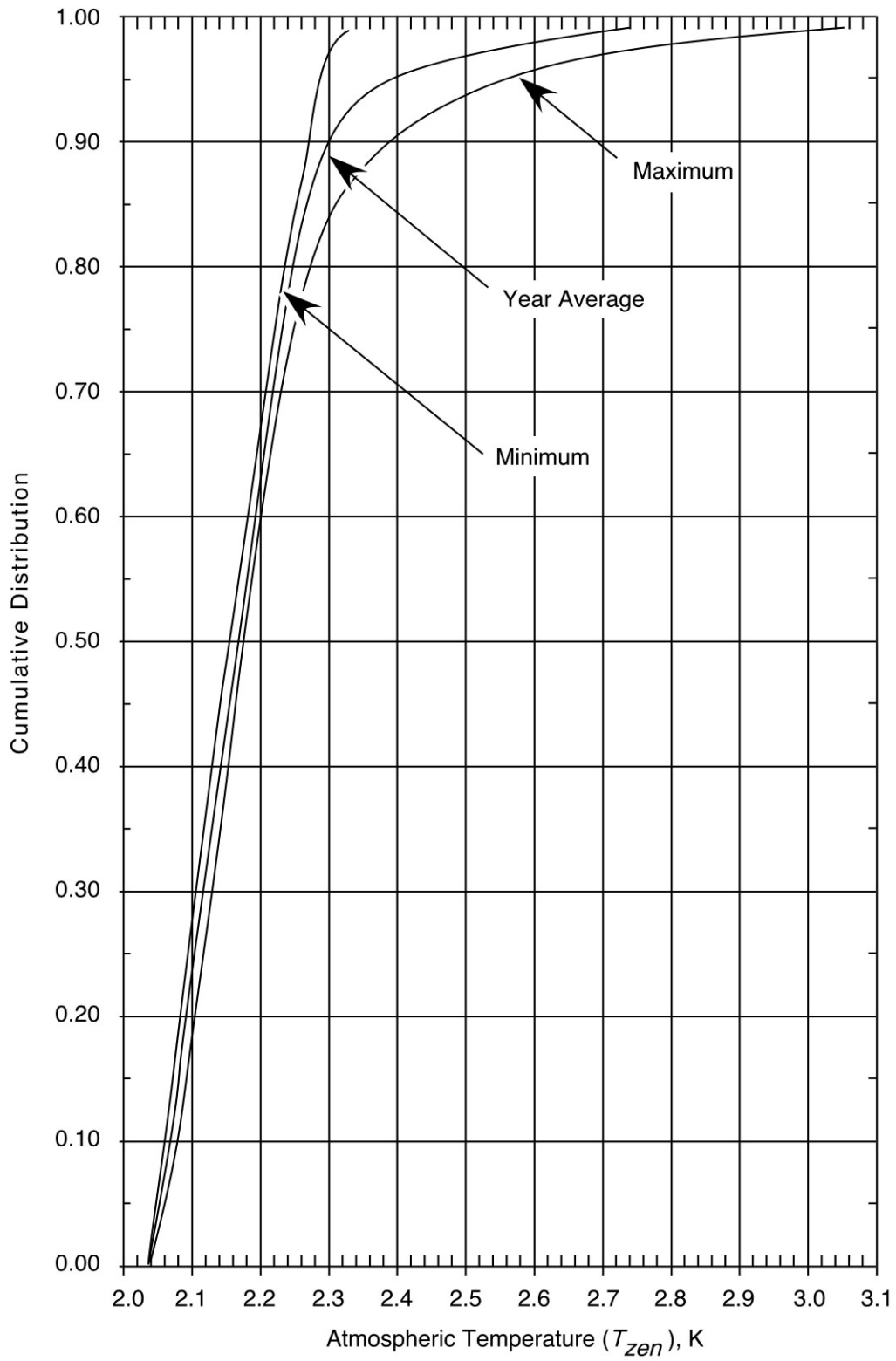
Figure 3. Cumulative Distributions of Zenith Atmospheric Noise Temperature
at L-Band and S-Band, Madrid DSCC
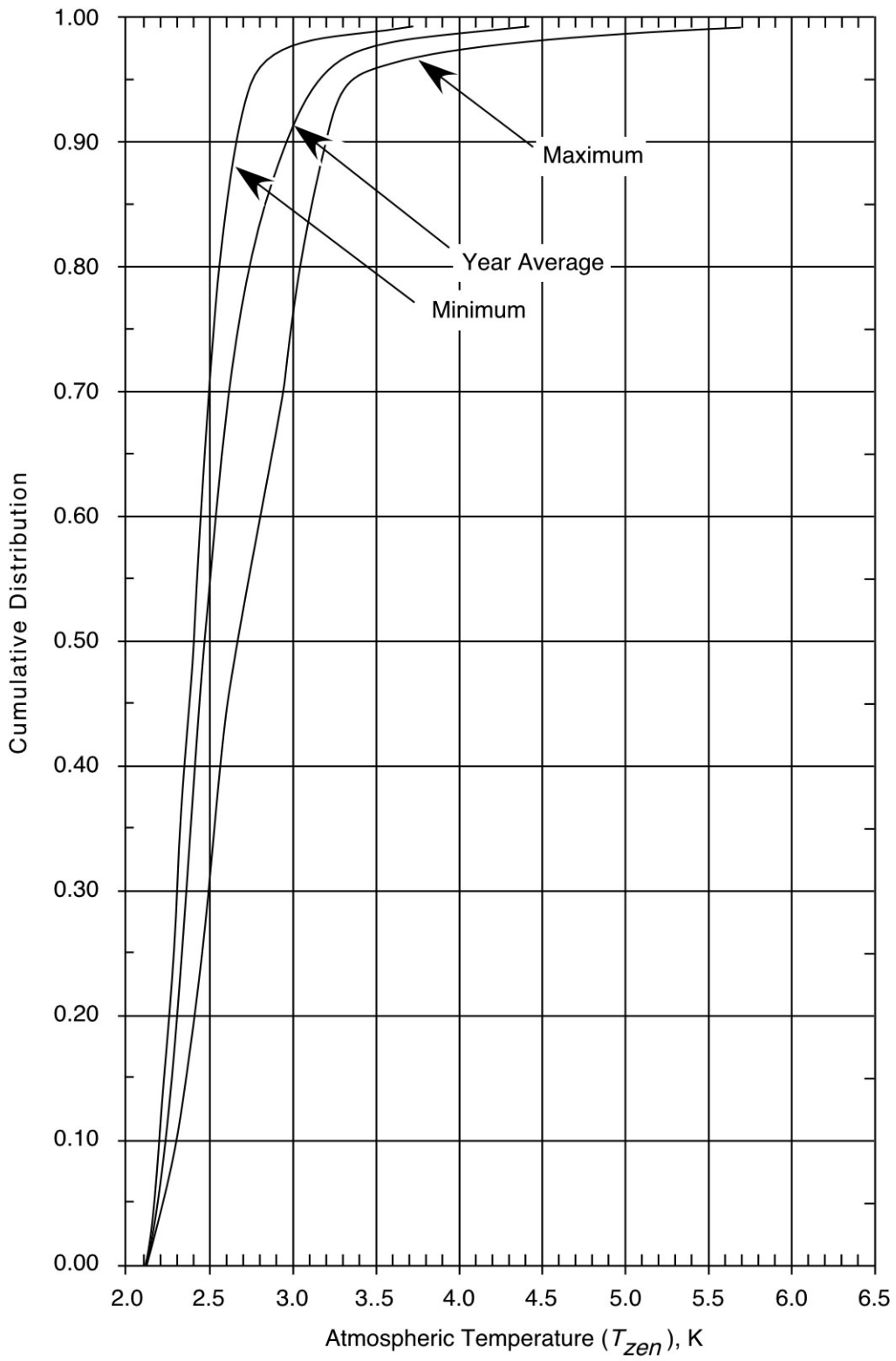
Figure 4.   Cumulative Distributions of Zenith Atmospheric Noise Temperature
at X-Band, Goldstone DSCC
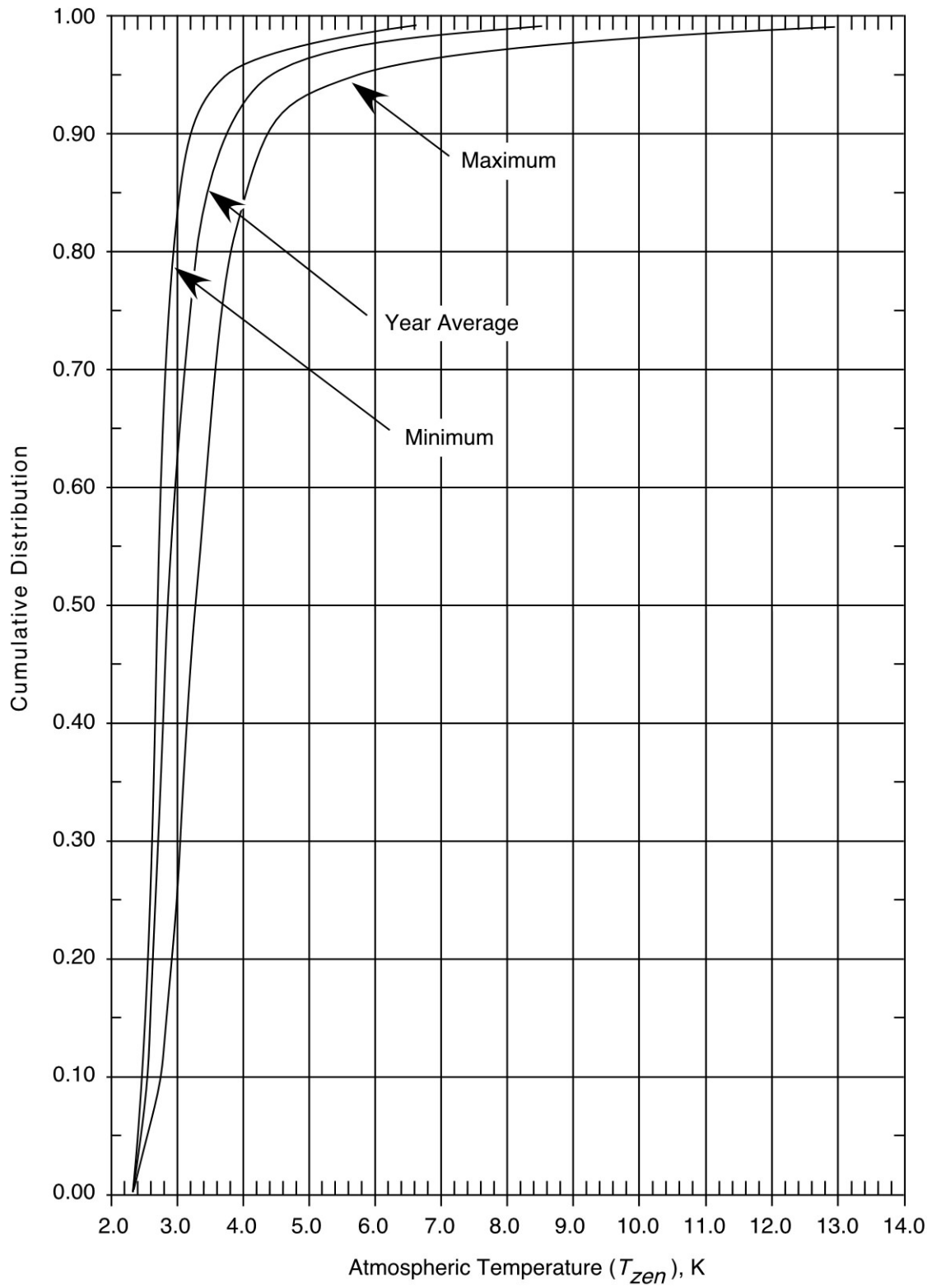
Figure 5.   Cumulative Distributions of Zenith Atmospheric Noise Temperature
at X-Band, Canberra DSCC
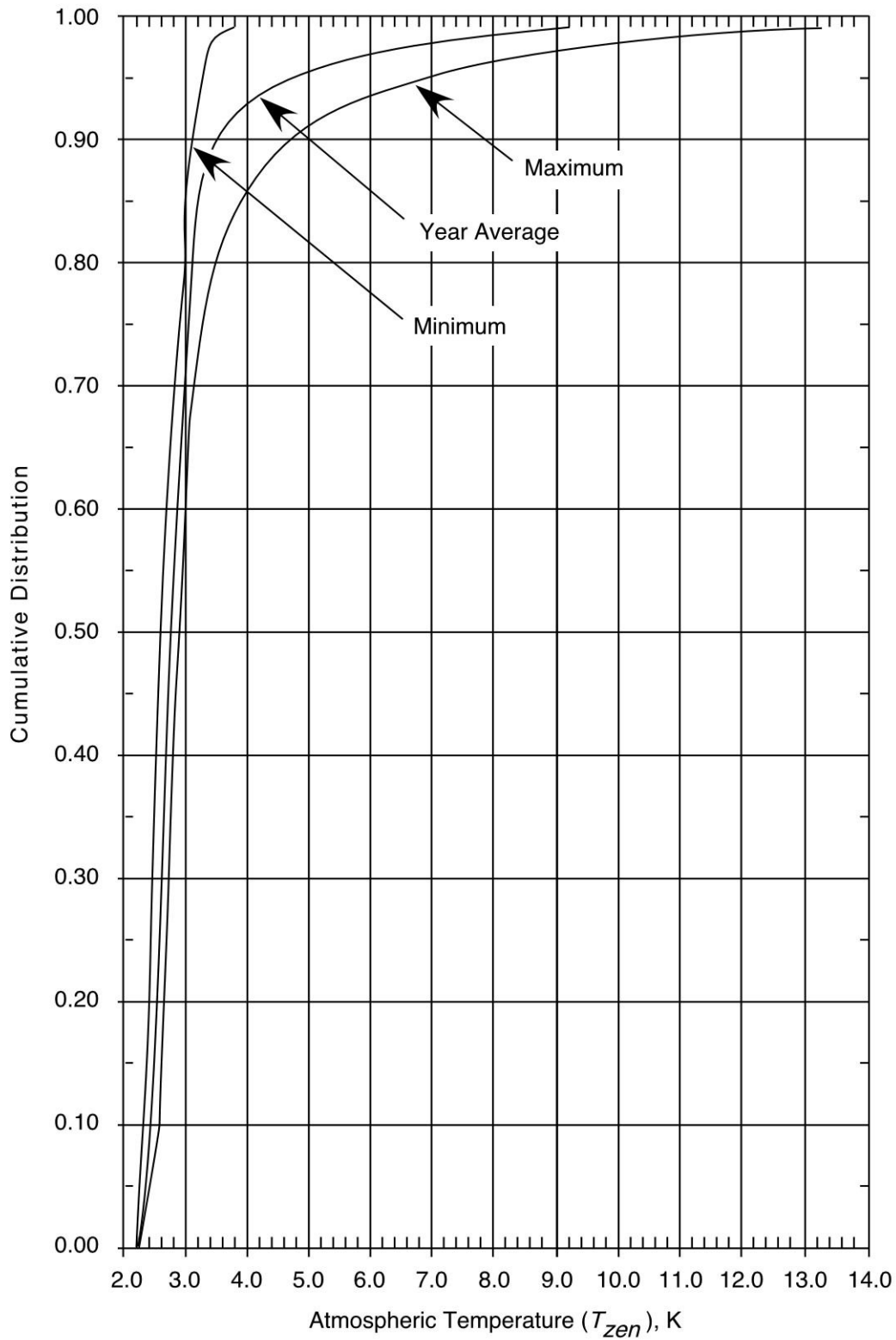
Figure 6.   Cumulative Distributions of Zenith Atmospheric Noise Temperature
at X-Band, Madrid DSCC
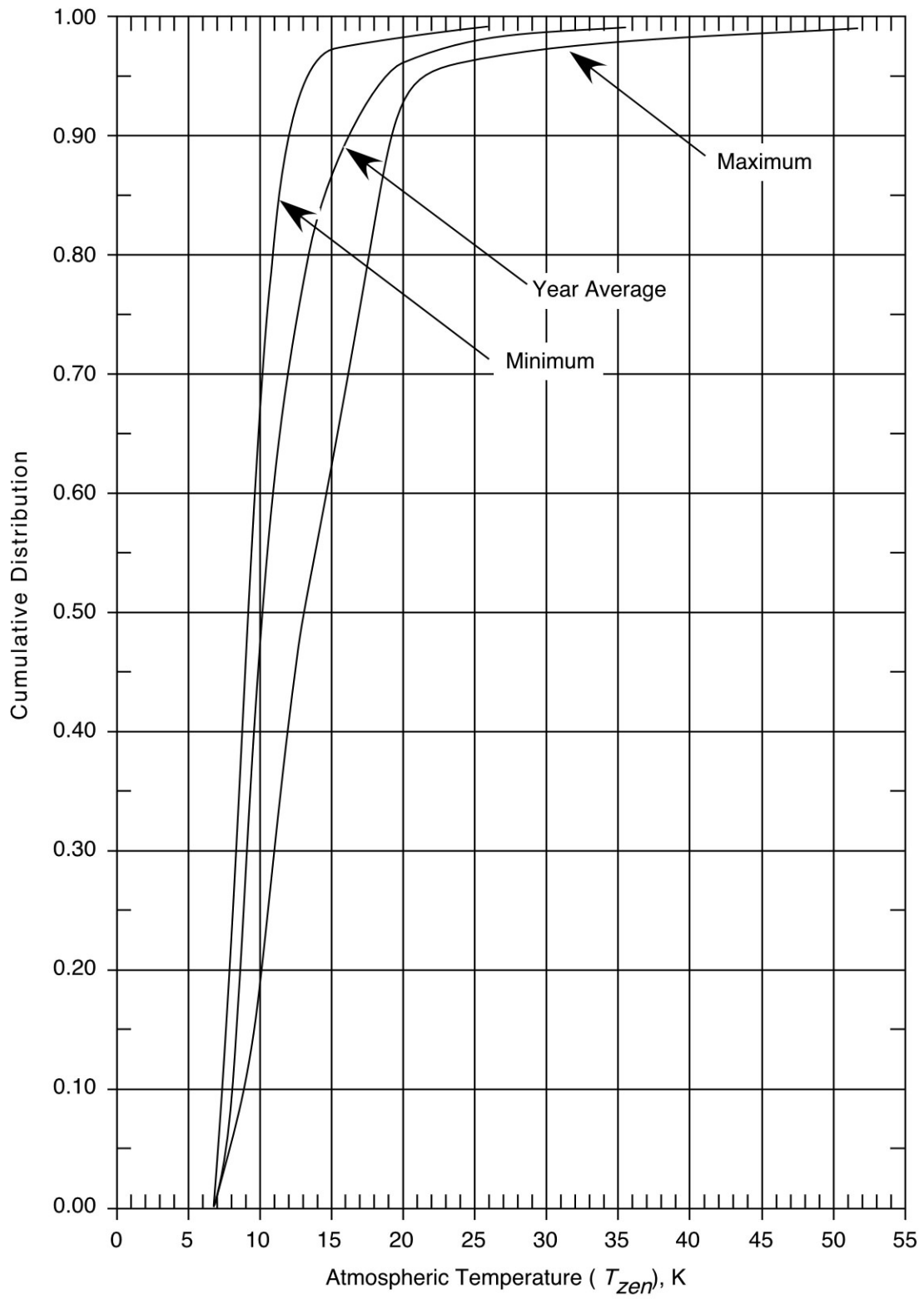
Figure 7.   Cumulative Distributions of Zenith Atmospheric Noise Temperature
at Ka-Band, Goldstone DSCC
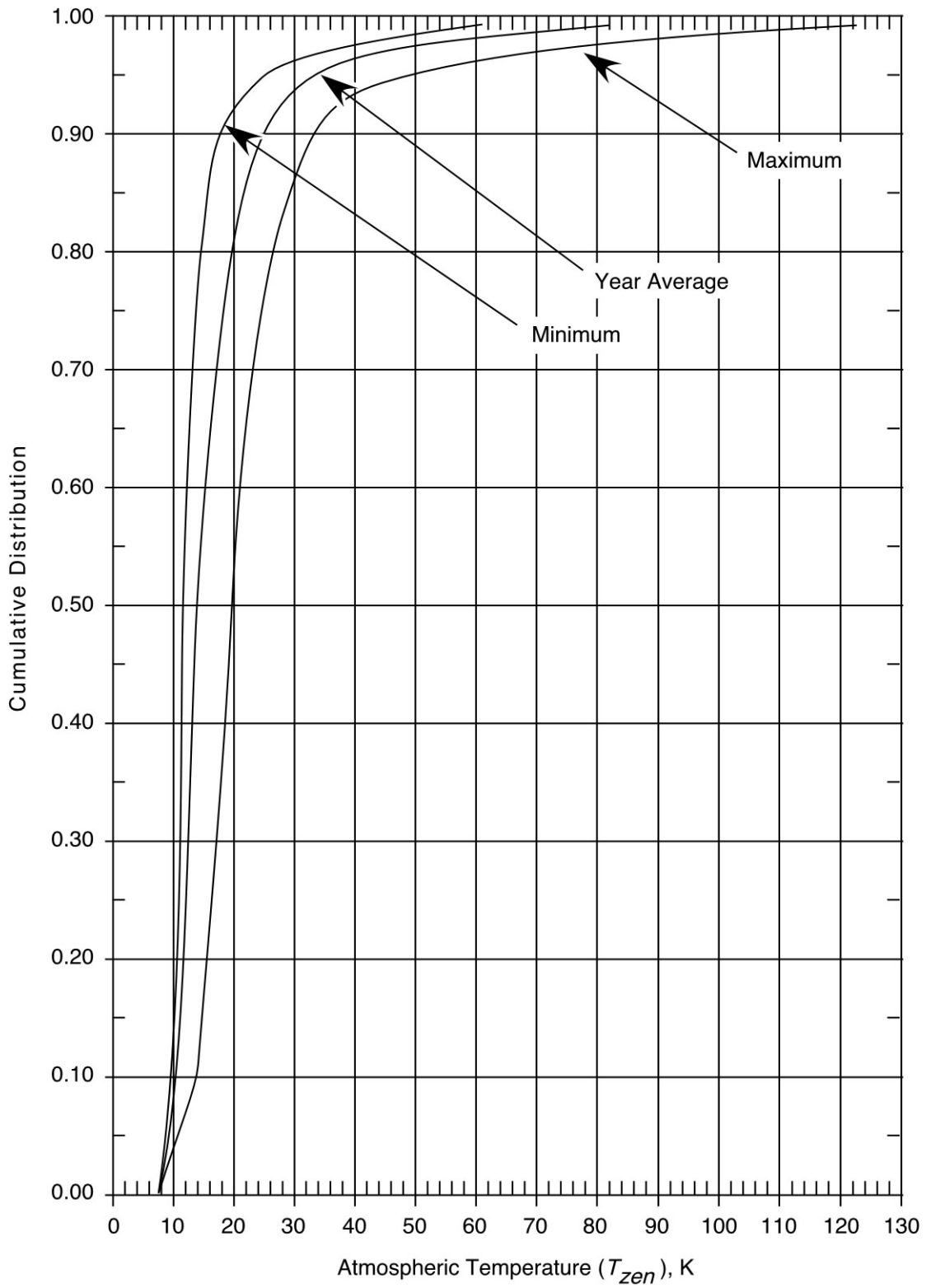
Figure 8.   Cumulative Distributions of Zenith Atmospheric Noise Temperature
at Ka-Band, Canberra DSCC
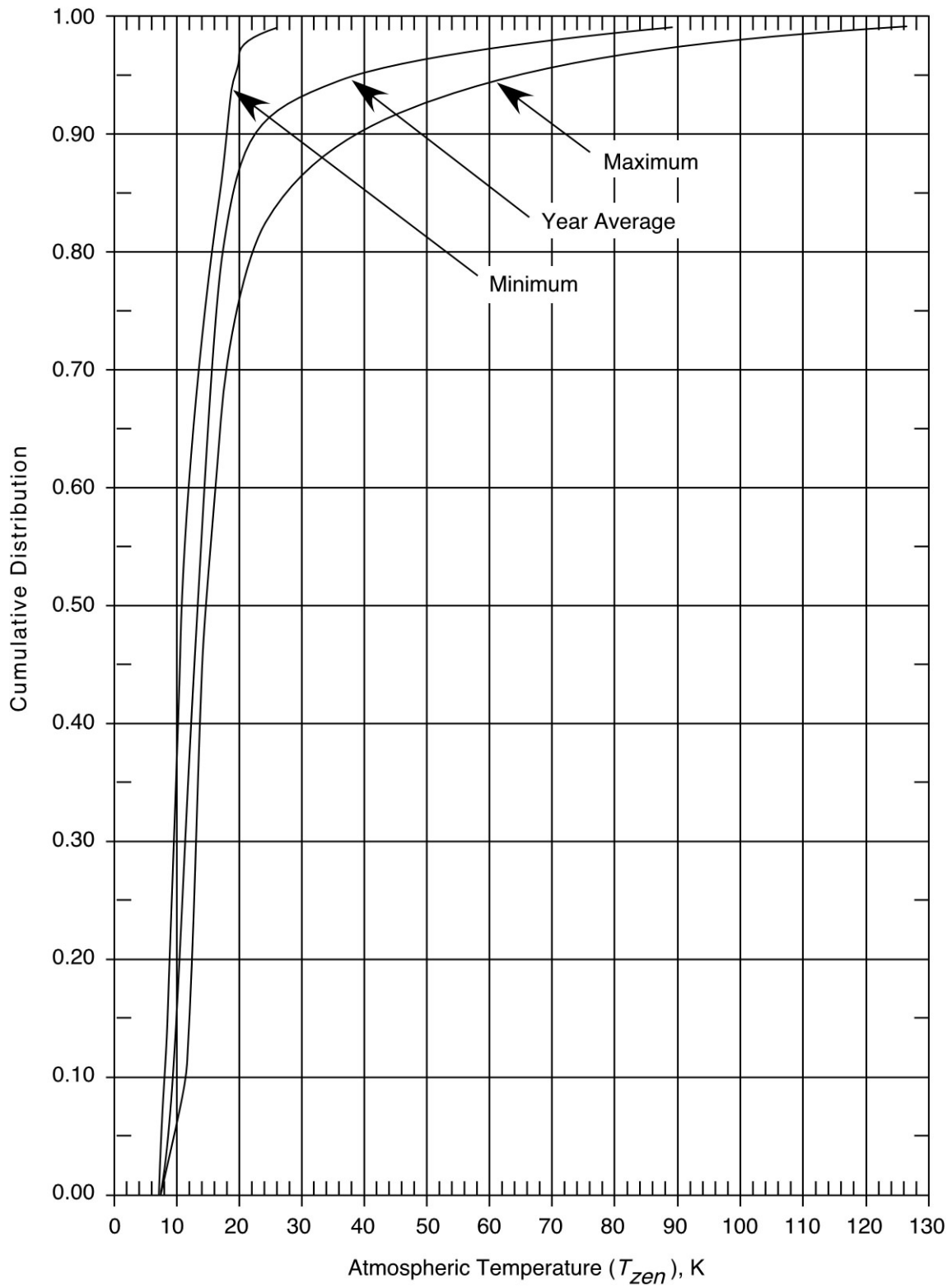
Figure 9.   Cumulative Distributions of Zenith Atmospheric Noise Temperature
at Ka-Band, Madrid DSCC
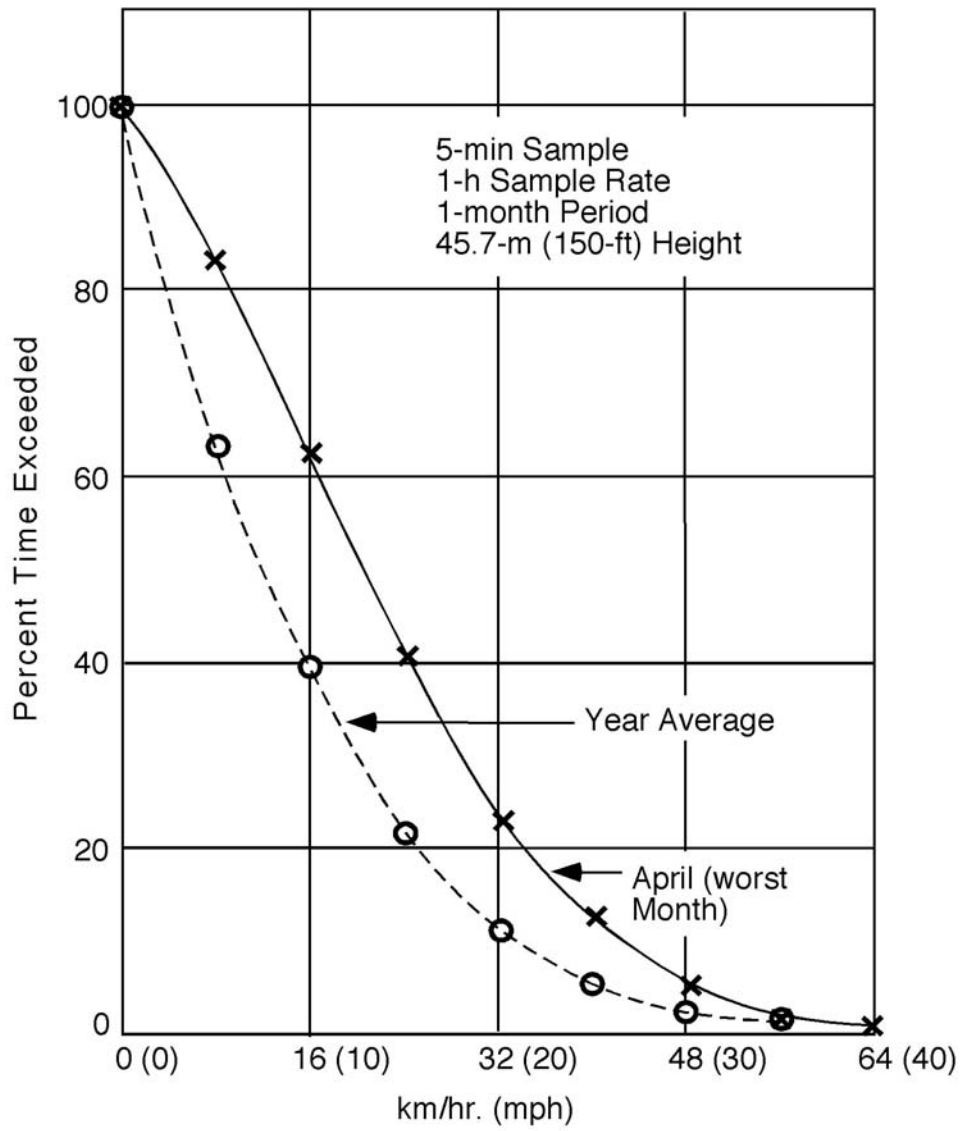
Figure 10. Probability Distribution of Wind Conditions at Goldstone
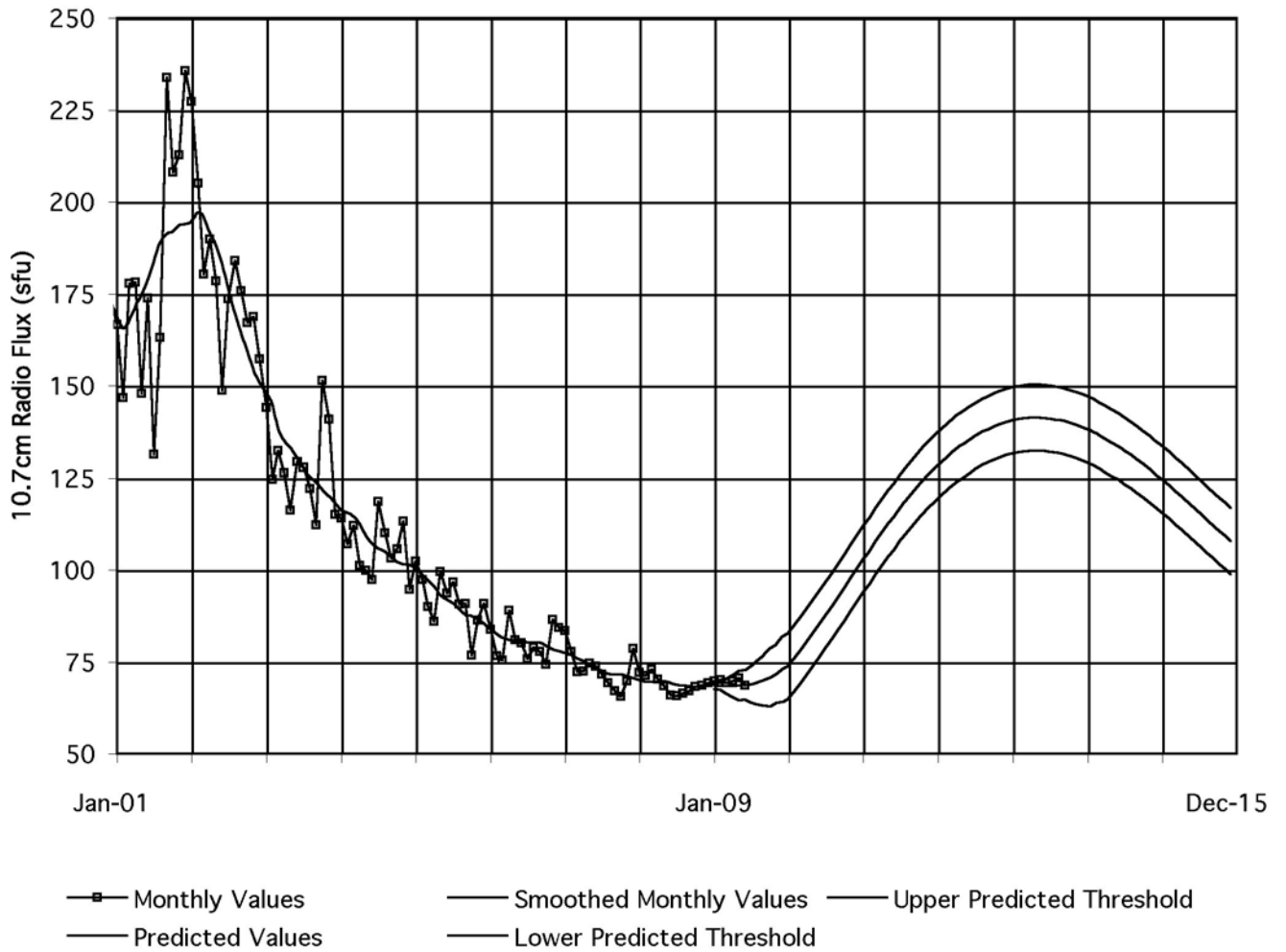
Figure 11.   Solar Radio Flux at 2800 MHz (10.7 cm wavelength) from 2001 through 2015
(Covering the end of Solar Cycle 23 and the beginning of-Solar Cycle 24) .
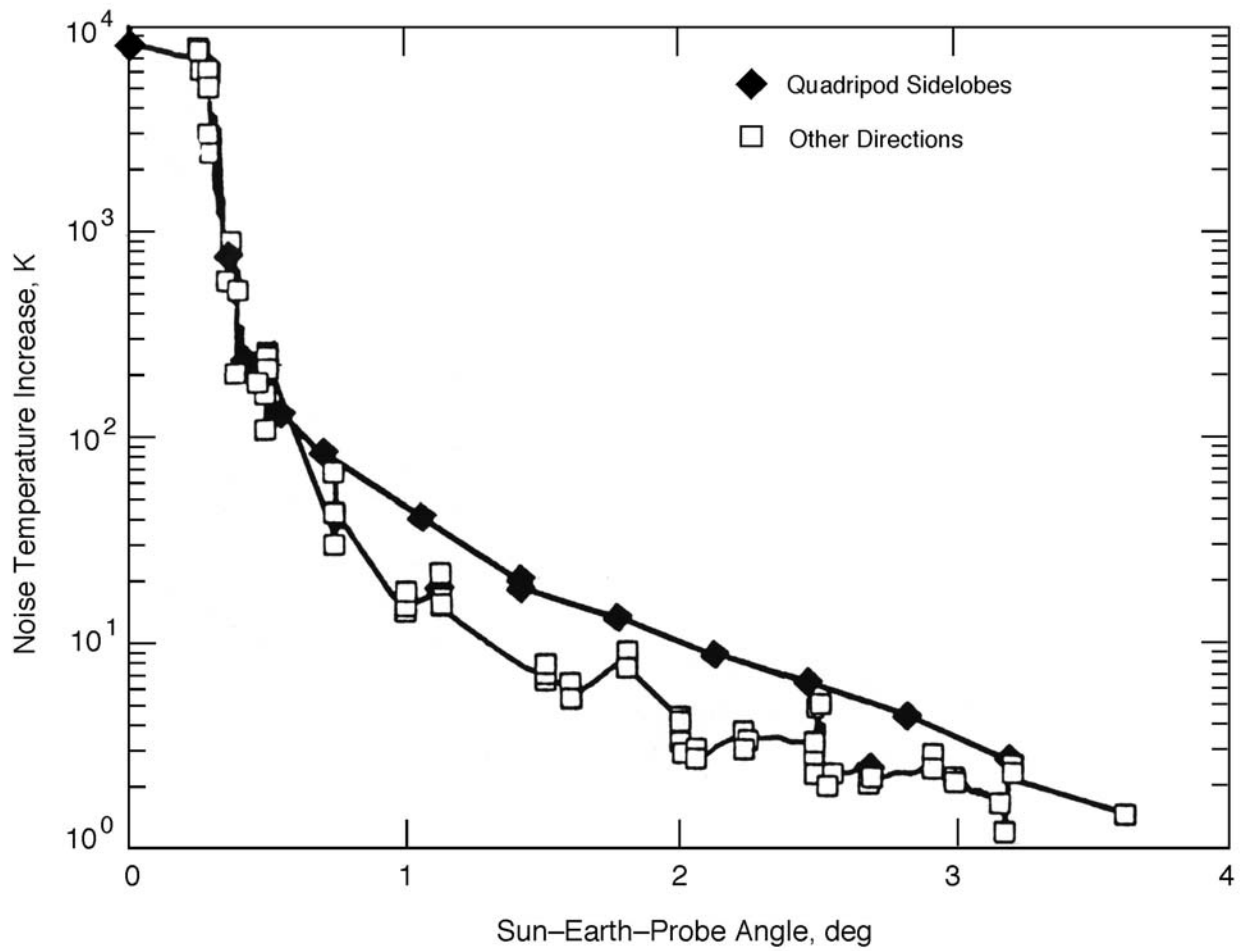
Figure 12. DSS-15 HEF Antenna X-Band System Noise Temperature Increases Due to the Sun at Various Offset Angles, Showing Larger Increases Perpendicular to Quadripod Directions
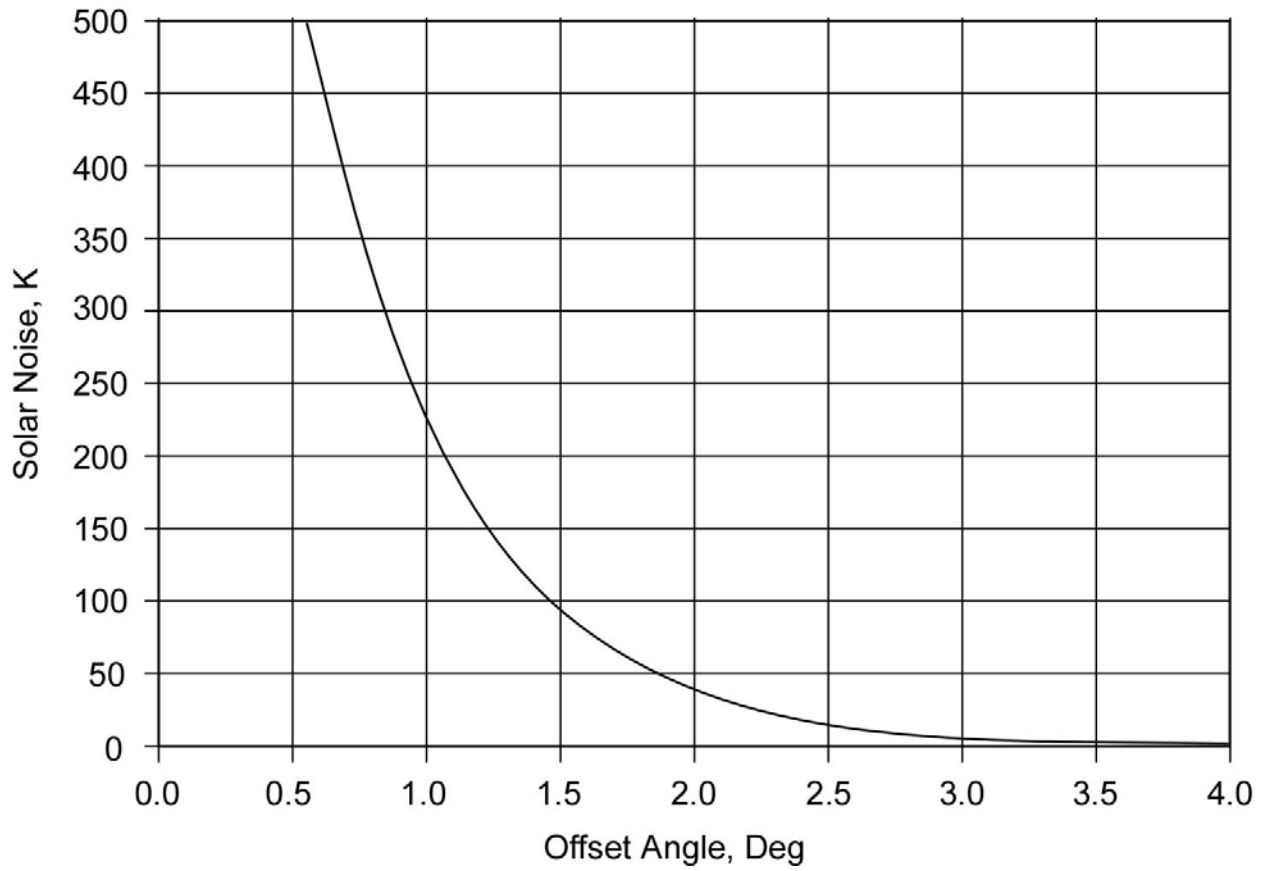
Figure 13. Solar Noise Contribution for a 34-Meter Antenna at S-band at Various Offset Angles from the Sun
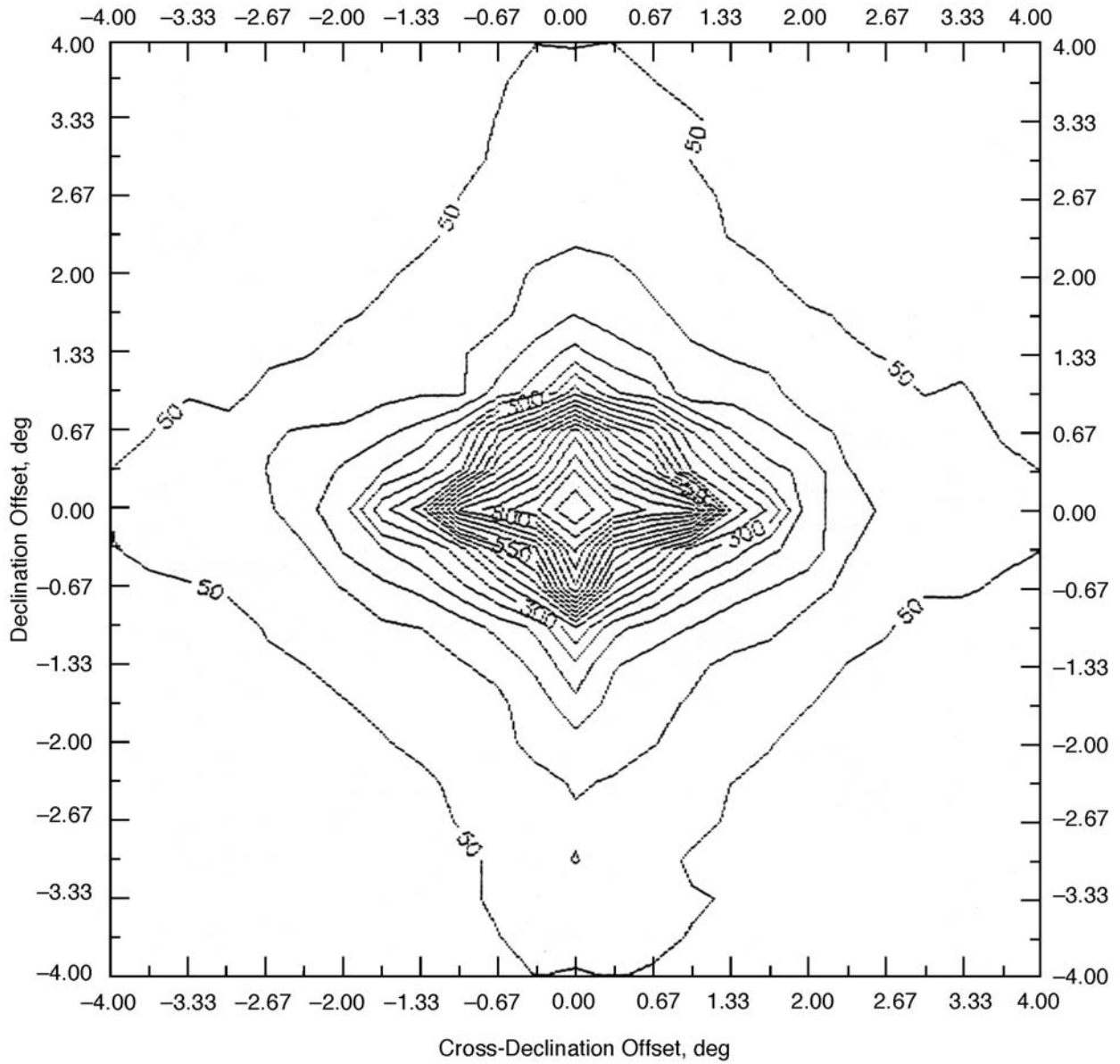
Figure 14. DSS-12 S-Band Total System Noise Temperature at Various Declination and Cross-
Declination Offsets from the Sun
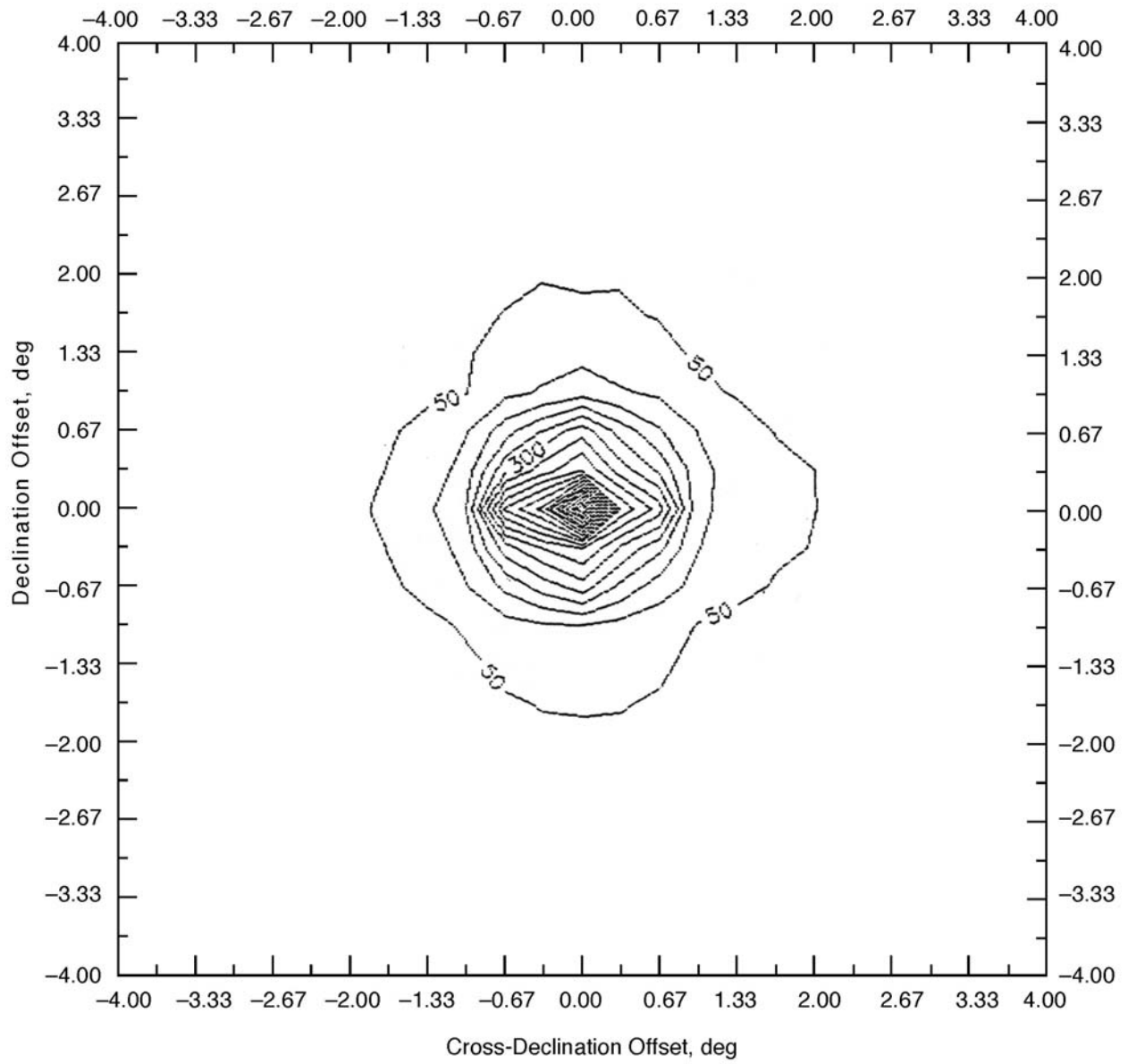
Figure 15. DSS-12 X-Band Total System Noise Temperature at Various Declination and Cross-Declination Offsets from the Sun
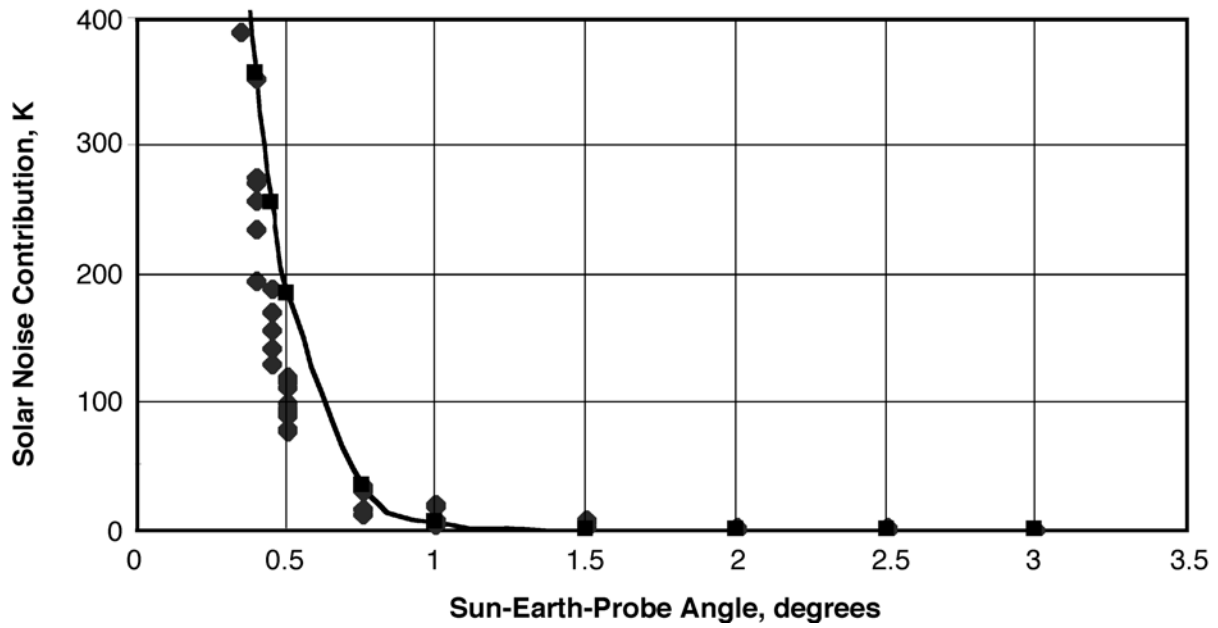
Figure 16. DSS-13 Beam-Waveguide Antenna X-Band Noise Temperature Increase Versus Offset Angle, March 1996
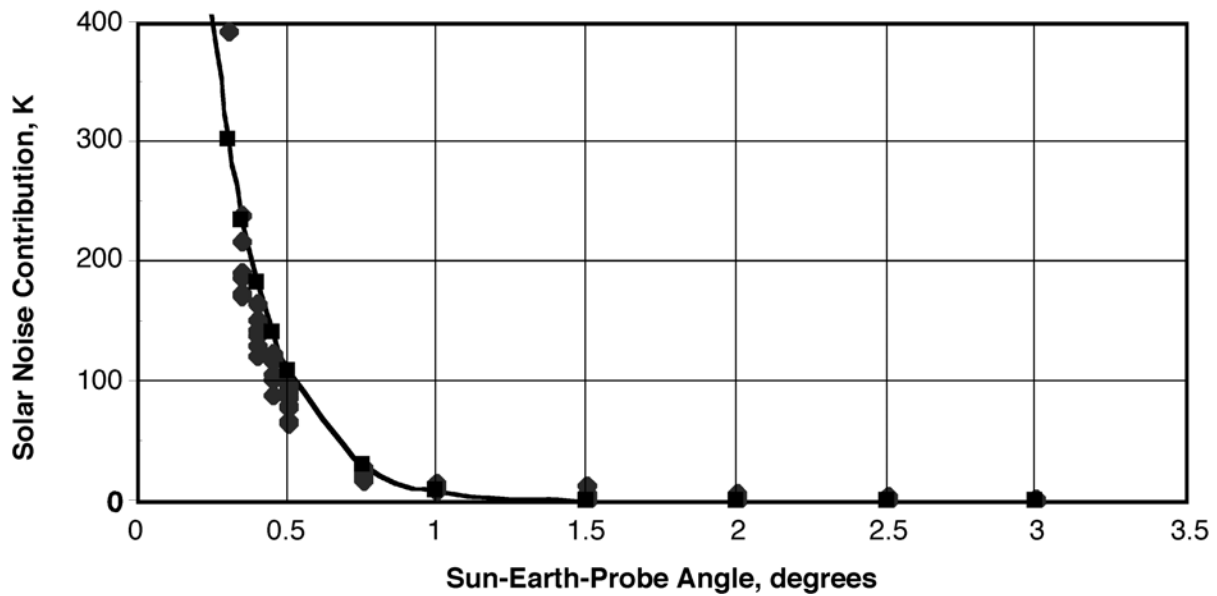
Figure 17. DSS-13 Beam-Waveguide Antenna Ka-Band Noise Temperature Increase Versus Offset Angle, March 1996
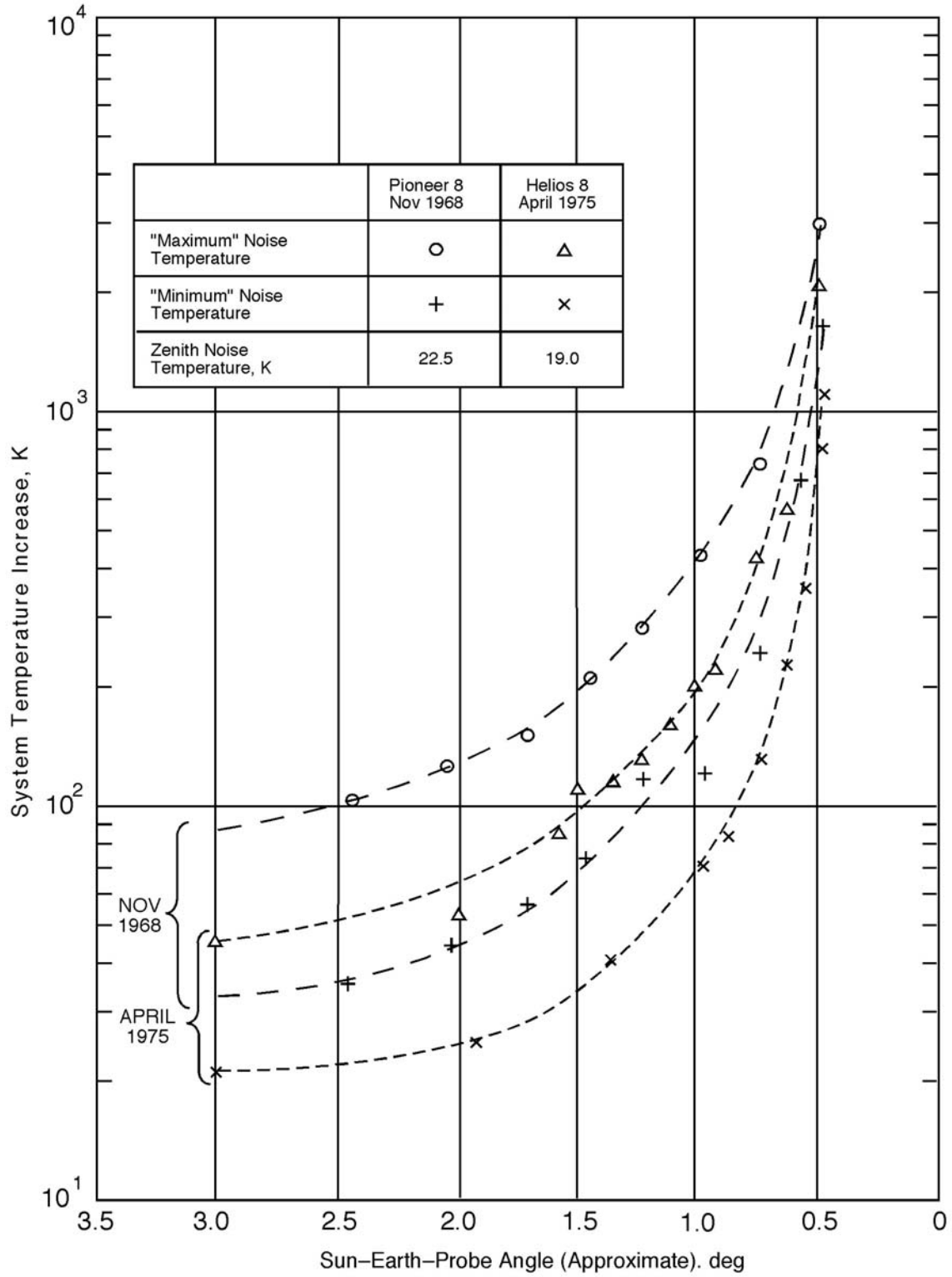
Figure 18. Total S-Band System Noise Temperature for 70-m Antennas Tracking Spacecraft Near the Sun (Derived from 64-m Measurements)
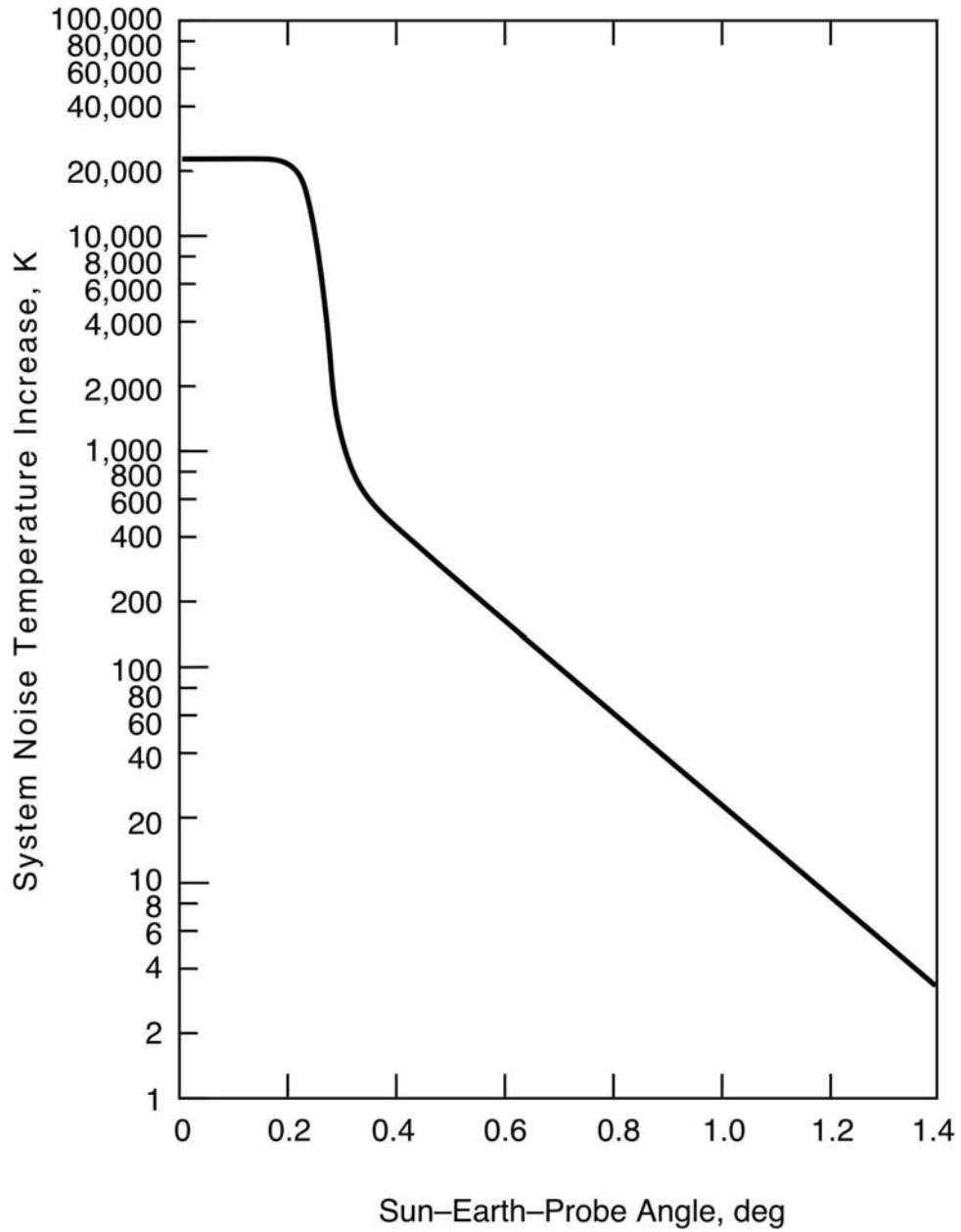
Figure 19. X-Band Noise Temperature Increase for 70-m Antennas as a Function of Sun-Earth-Probe Angle, Nominal Sun, 23,000 K Disk Temperature
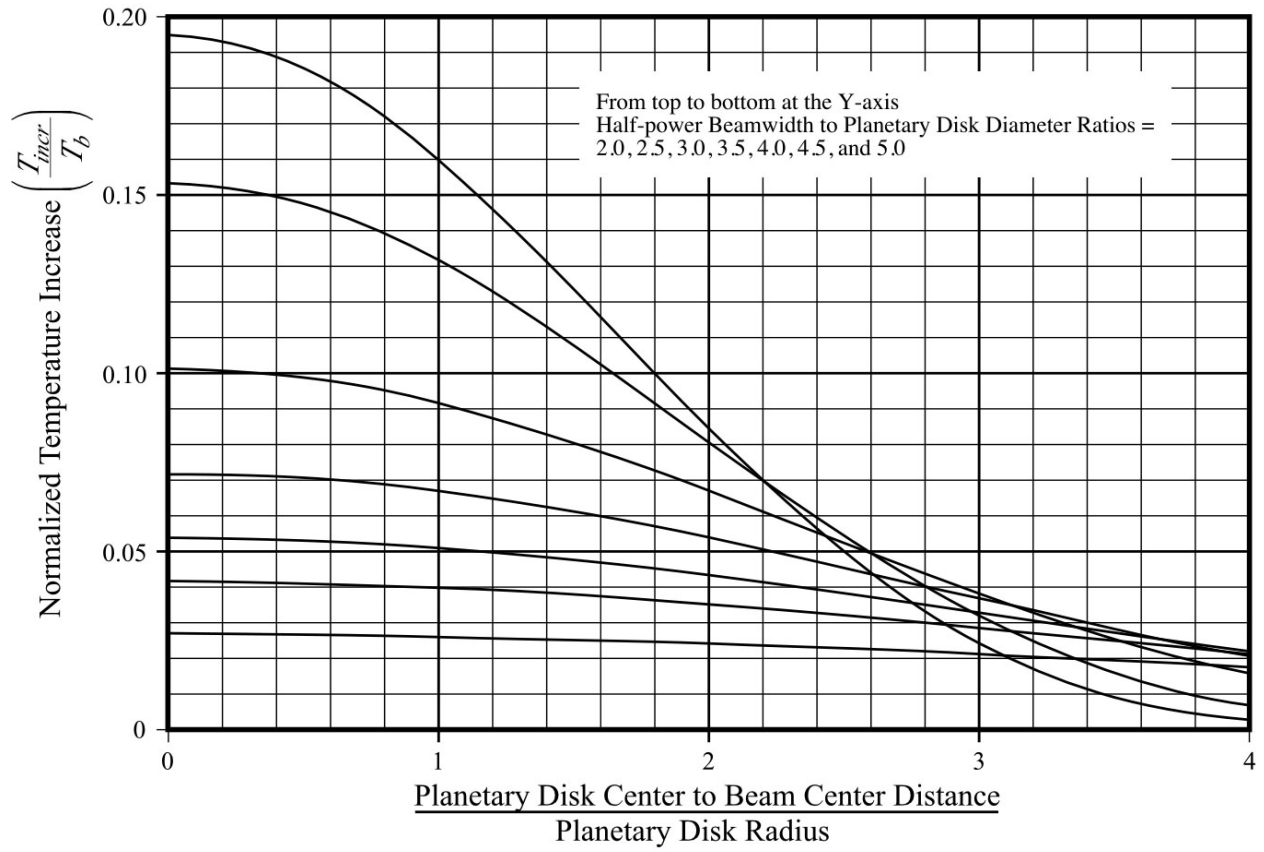
Figure 20. Normalized Temperature Increase for Half-power Beamwidth to Planetary
Disk Diameter Ratios from 2.0 to 5.0

Table 1. Cumulative Distributions of Zenith Atmospheric Noise Temperature at
L- and S-Bands for Goldstone DSCC, K

CD	January	February	March	April	May	June
0.00	1.948	1.948	1.948	1.948	1.948	1.948
0.10	1.970	1.971	1.972	1.973	1.975	1.974
0.20	1.992	1.992	1.993	1.994	1.996	1.997
0.25	2.002	2.002	2.003	2.004	2.007	2.007
0.30	2.013	2.013	2.014	2.015	2.018	2.018
0.40	2.034	2.034	2.035	2.036	2.039	2.040
0.50	2.055	2.055	2.055	2.056	2.060	2.062
0.60	2.076	2.076	2.076	2.077	2.081	2.084
0.70	2.098	2.098	2.097	2.099	2.104	2.108
0.80	2.122	2.122	2.119	2.120	2.128	2.135
0.85	2.136	2.136	2.132	2.132	2.141	2.148
0.90	2.153	2.154	2.145	2.144	2.155	2.162
0.92	2.162	2.165	2.151	2.150	2.162	2.169
0.93	2.168	2.174	2.155	2.153	2.166	2.172
0.94	2.177	2.185	2.160	2.156	2.171	2.177
0.95	2.189	2.200	2.164	2.160	2.177	2.181
0.96	2.206	2.222	2.173	2.166	2.186	2.188
0.97	2.231	2.250	2.187	2.174	2.197	2.196
0.98	2.271	2.298	2.211	2.191	2.226	2.217
0.99	2.366	2.389	2.276	2.240	2.273	2.268

Table 1 (Cont'd). Cumulative Distributions of Zenith Atmospheric Noise Temperature at
L- and S-Bands for Goldstone DSCC, K

CD	July	August	September	October	November	December	Minimum	Year Average	Maximum
0.00	1.948	1.948	1.948	1.948	1.948	1.948	1.948	1.948	1.948
0.10	1.978	1.978	1.976	1.975	1.972	1.971	1.970	1.973	1.978
0.20	2.002	2.002	1.998	1.997	1.993	1.992	1.992	1.995	2.002
0.25	2.014	2.013	2.009	2.008	2.004	2.003	2.002	2.006	2.014
0.30	2.026	2.025	2.020	2.018	2.014	2.013	2.013	2.016	2.026
0.40	2.049	2.049	2.041	2.040	2.036	2.034	2.034	2.038	2.049
0.50	2.075	2.074	2.064	2.061	2.057	2.055	2.055	2.059	2.075
0.60	2.103	2.099	2.088	2.083	2.079	2.076	2.076	2.082	2.103
0.70	2.129	2.125	2.113	2.105	2.102	2.099	2.097	2.105	2.129
0.80	2.155	2.151	2.142	2.129	2.126	2.123	2.119	2.132	2.155
0.85	2.169	2.166	2.157	2.141	2.140	2.137	2.132	2.148	2.169
0.90	2.183	2.183	2.174	2.156	2.155	2.152	2.144	2.167	2.183
0.92	2.190	2.190	2.181	2.163	2.163	2.160	2.150	2.175	2.190
0.93	2.194	2.193	2.185	2.167	2.168	2.164	2.153	2.180	2.194
0.94	2.198	2.198	2.189	2.172	2.172	2.171	2.156	2.185	2.198
0.95	2.204	2.202	2.193	2.177	2.177	2.180	2.160	2.191	2.204
0.96	2.211	2.208	2.198	2.183	2.183	2.193	2.166	2.198	2.222
0.97	2.220	2.215	2.205	2.191	2.194	2.215	2.174	2.209	2.250
0.98	2.239	2.231	2.218	2.208	2.220	2.250	2.191	2.232	2.298
0.99	2.289	2.253	2.261	2.261	2.290	2.356	2.240	2.291	2.389

Table 2. Cumulative Distributions of Zenith Atmospheric Noise Temperature at
L- and S-Bands for Canberra DSCC, K

CD	January	February	March	April	May	June
0.00	2.076	2.076	2.076	2.076	2.076	2.076
0.10	2.121	2.131	2.122	2.115	2.113	2.109
0.20	2.149	2.159	2.149	2.141	2.137	2.132
0.25	2.162	2.173	2.161	2.153	2.148	2.144
0.30	2.175	2.187	2.174	2.165	2.160	2.155
0.40	2.202	2.214	2.200	2.189	2.183	2.178
0.50	2.228	2.242	2.226	2.213	2.205	2.202
0.60	2.256	2.269	2.254	2.238	2.229	2.227
0.70	2.286	2.299	2.282	2.264	2.253	2.254
0.80	2.321	2.337	2.314	2.292	2.282	2.284
0.85	2.342	2.363	2.333	2.308	2.299	2.301
0.90	2.368	2.397	2.359	2.329	2.325	2.328
0.92	2.385	2.421	2.371	2.342	2.341	2.346
0.93	2.396	2.439	2.378	2.350	2.351	2.359
0.94	2.409	2.469	2.388	2.361	2.363	2.376
0.95	2.427	2.510	2.402	2.377	2.378	2.404
0.96	2.452	2.571	2.424	2.400	2.398	2.443
0.97	2.504	2.657	2.458	2.429	2.427	2.494
0.98	2.606	2.785	2.520	2.480	2.479	2.567
0.99	2.787	3.064	2.657	2.591	2.590	2.693

Table 2 (Cont'd). Cumulative Distributions of Zenith Atmospheric Noise Temperature at
L- and S-Bands for Canberra DSCC, K

CD	July	August	September	October	November	December	Minimum	Year Average	Maximum
0.00	2.076	2.076	2.076	2.076	2.076	2.076	2.076	2.076	2.076
0.10	2.108	2.108	2.110	2.111	2.118	2.117	2.108	2.112	2.131
0.20	2.132	2.131	2.134	2.136	2.143	2.144	2.131	2.136	2.159
0.25	2.143	2.142	2.146	2.147	2.156	2.157	2.142	2.149	2.173
0.30	2.154	2.153	2.158	2.159	2.168	2.170	2.153	2.161	2.187
0.40	2.177	2.176	2.181	2.183	2.194	2.195	2.176	2.185	2.214
0.50	2.199	2.198	2.204	2.206	2.219	2.221	2.198	2.211	2.242
0.60	2.223	2.221	2.228	2.230	2.247	2.249	2.221	2.237	2.269
0.70	2.248	2.246	2.253	2.256	2.277	2.277	2.246	2.267	2.299
0.80	2.276	2.272	2.281	2.287	2.313	2.312	2.272	2.300	2.337
0.85	2.293	2.288	2.298	2.307	2.336	2.333	2.288	2.322	2.363
0.90	2.317	2.311	2.323	2.335	2.375	2.366	2.311	2.350	2.397
0.92	2.331	2.325	2.340	2.353	2.402	2.386	2.325	2.367	2.421
0.93	2.341	2.336	2.351	2.365	2.423	2.398	2.336	2.378	2.439
0.94	2.354	2.348	2.364	2.381	2.447	2.417	2.348	2.393	2.469
0.95	2.370	2.366	2.383	2.402	2.478	2.444	2.366	2.411	2.510
0.96	2.393	2.391	2.413	2.431	2.528	2.483	2.391	2.440	2.571
0.97	2.424	2.433	2.458	2.471	2.601	2.550	2.424	2.487	2.657
0.98	2.481	2.506	2.521	2.541	2.705	2.655	2.479	2.567	2.785
0.99	2.585	2.637	2.681	2.704	2.893	2.857	2.585	2.730	3.064

Table 3. Cumulative Distributions of Zenith Atmospheric Noise Temperature at
L- and S-Bands for Madrid DSCC, K

CD	January	February	March	April	May	June
0.00	2.035	2.035	2.035	2.035	2.035	2.035
0.10	2.059	2.060	2.064	2.067	2.073	2.075
0.20	2.083	2.084	2.087	2.090	2.097	2.100
0.25	2.095	2.095	2.099	2.102	2.109	2.113
0.30	2.106	2.107	2.111	2.114	2.121	2.125
0.40	2.129	2.129	2.134	2.137	2.145	2.149
0.50	2.153	2.153	2.157	2.161	2.169	2.172
0.60	2.178	2.177	2.181	2.185	2.193	2.196
0.70	2.206	2.203	2.206	2.209	2.219	2.221
0.80	2.240	2.236	2.238	2.239	2.248	2.247
0.85	2.264	2.261	2.261	2.261	2.268	2.260
0.90	2.309	2.313	2.306	2.305	2.307	2.276
0.92	2.343	2.354	2.338	2.335	2.336	2.284
0.93	2.367	2.380	2.360	2.356	2.356	2.289
0.94	2.400	2.411	2.387	2.383	2.381	2.295
0.95	2.438	2.448	2.422	2.419	2.413	2.305
0.96	2.485	2.493	2.466	2.461	2.457	2.318
0.97	2.543	2.547	2.528	2.518	2.512	2.342
0.98	2.616	2.630	2.608	2.597	2.597	2.397
0.99	2.736	2.847	2.738	2.723	2.770	2.532

Table 3 (Cont'd). Cumulative Distributions of Zenith Atmospheric Noise Temperature at
L- and S-Bands for Madrid DSCC, K

CD	July	August	September	October	November	December	Minimum	Year Average	Maximum
0.00	2.035	2.035	2.035	2.035	2.035	2.035	2.035	2.035	2.035
0.10	2.077	2.077	2.074	2.072	2.063	2.062	2.059	2.066	2.077
0.20	2.101	2.102	2.100	2.098	2.087	2.086	2.083	2.091	2.102
0.25	2.113	2.114	2.112	2.110	2.099	2.097	2.095	2.103	2.114
0.30	2.124	2.126	2.124	2.122	2.111	2.109	2.106	2.116	2.126
0.40	2.147	2.150	2.148	2.147	2.134	2.132	2.129	2.140	2.150
0.50	2.170	2.173	2.172	2.173	2.158	2.156	2.153	2.165	2.173
0.60	2.194	2.196	2.196	2.199	2.183	2.182	2.177	2.190	2.199
0.70	2.217	2.220	2.221	2.228	2.211	2.211	2.203	2.217	2.228
0.80	2.242	2.245	2.248	2.269	2.246	2.248	2.236	2.246	2.269
0.85	2.255	2.258	2.263	2.307	2.272	2.274	2.255	2.263	2.307
0.90	2.268	2.272	2.280	2.381	2.330	2.322	2.268	2.293	2.381
0.92	2.274	2.278	2.291	2.433	2.379	2.356	2.274	2.317	2.433
0.93	2.278	2.281	2.298	2.467	2.411	2.380	2.278	2.335	2.467
0.94	2.282	2.285	2.306	2.510	2.448	2.412	2.282	2.360	2.510
0.95	2.286	2.290	2.318	2.557	2.487	2.453	2.286	2.393	2.557
0.96	2.290	2.296	2.335	2.617	2.537	2.501	2.290	2.440	2.617
0.97	2.295	2.305	2.365	2.697	2.596	2.563	2.295	2.500	2.697
0.98	2.304	2.324	2.430	2.824	2.678	2.650	2.304	2.587	2.824
0.99	2.332	2.388	2.579	3.053	2.830	2.805	2.332	2.741	3.053

Table 4. Cumulative Distributions of Zenith Atmospheric Noise Temperature at X-Band
for Goldstone DSCC, K

CD	January	February	March	April	May	June
0.00	2.140	2.140	2.140	2.140	2.140	2.140
0.10	2.205	2.212	2.228	2.239	2.269	2.261
0.20	2.261	2.262	2.276	2.289	2.321	2.324
0.25	2.284	2.284	2.298	2.312	2.347	2.351
0.30	2.307	2.308	2.320	2.335	2.371	2.378
0.40	2.352	2.356	2.365	2.379	2.418	2.433
0.50	2.398	2.401	2.407	2.421	2.465	2.496
0.60	2.450	2.450	2.450	2.466	2.519	2.562
0.70	2.506	2.511	2.498	2.516	2.585	2.650
0.80	2.594	2.599	2.563	2.574	2.673	2.766
0.85	2.667	2.668	2.607	2.613	2.731	2.829
0.90	2.776	2.792	2.669	2.662	2.809	2.901
0.92	2.851	2.893	2.708	2.690	2.852	2.940
0.93	2.913	2.990	2.739	2.706	2.880	2.968
0.94	3.003	3.117	2.771	2.727	2.925	2.999
0.95	3.137	3.296	2.813	2.760	2.983	3.036
0.96	3.353	3.558	2.901	2.807	3.073	3.104
0.97	3.656	3.907	3.071	2.896	3.202	3.193
0.98	4.171	4.526	3.364	3.094	3.563	3.441
0.99	5.418	5.722	4.215	3.728	4.180	4.106

Table 4 (Cont'd). Cumulative Distributions of Zenith Atmospheric Noise Temperature at
X-Band for Goldstone DSCC, K

CD	July	August	September	October	November	December	Minimum	Year Average	Maximum
0.00	2.140	2.140	2.140	2.140	2.140	2.140	2.140	2.140	2.140
0.10	2.311	2.313	2.287	2.264	2.228	2.214	2.205	2.243	2.313
0.20	2.404	2.395	2.348	2.331	2.280	2.266	2.261	2.302	2.404
0.25	2.447	2.432	2.374	2.358	2.305	2.290	2.284	2.329	2.447
0.30	2.486	2.471	2.400	2.383	2.330	2.313	2.307	2.355	2.486
0.40	2.562	2.562	2.455	2.431	2.381	2.358	2.352	2.407	2.562
0.50	2.667	2.663	2.522	2.482	2.435	2.402	2.398	2.462	2.667
0.60	2.806	2.765	2.608	2.537	2.493	2.452	2.450	2.527	2.806
0.70	2.930	2.877	2.710	2.600	2.562	2.520	2.498	2.610	2.930
0.80	3.042	2.991	2.863	2.687	2.651	2.610	2.563	2.735	3.042
0.85	3.108	3.072	2.955	2.737	2.717	2.675	2.607	2.831	3.108
0.90	3.186	3.177	3.055	2.818	2.808	2.770	2.662	2.963	3.186
0.92	3.226	3.221	3.107	2.868	2.863	2.824	2.690	3.028	3.226
0.93	3.256	3.248	3.133	2.900	2.904	2.861	2.706	3.068	3.256
0.94	3.294	3.283	3.162	2.935	2.943	2.920	2.727	3.116	3.294
0.95	3.342	3.320	3.197	2.976	2.983	3.018	2.760	3.170	3.342
0.96	3.410	3.371	3.242	3.034	3.033	3.179	2.807	3.238	3.558
0.97	3.514	3.447	3.307	3.124	3.167	3.440	2.896	3.358	3.907
0.98	3.748	3.640	3.465	3.327	3.494	3.889	3.094	3.650	4.526
0.99	4.385	3.905	4.013	4.009	4.396	5.275	3.728	4.421	5.722

Table 5. Cumulative Distributions of Zenith Atmospheric Noise Temperature at X-Band
for Canberra DSCC, K

CD	January	February	March	April	May	June
0.00	2.280	2.280	2.280	2.280	2.280	2.280
0.10	2.636	2.764	2.648	2.555	2.526	2.478
0.20	2.757	2.899	2.758	2.652	2.594	2.536
0.25	2.810	2.960	2.802	2.690	2.624	2.564
0.30	2.860	3.023	2.847	2.723	2.652	2.590
0.40	2.963	3.136	2.937	2.788	2.708	2.650
0.50	3.068	3.250	3.044	2.861	2.764	2.718
0.60	3.188	3.372	3.162	2.953	2.823	2.807
0.70	3.344	3.525	3.295	3.053	2.903	2.916
0.80	3.562	3.781	3.475	3.177	3.036	3.060
0.85	3.715	4.006	3.603	3.265	3.148	3.170
0.90	3.948	4.335	3.816	3.425	3.363	3.405
0.92	4.125	4.594	3.933	3.543	3.529	3.603
0.93	4.245	4.818	4.004	3.626	3.641	3.741
0.94	4.391	5.193	4.108	3.753	3.774	3.948
0.95	4.603	5.718	4.273	3.942	3.949	4.293
0.96	4.912	6.504	4.542	4.225	4.191	4.797
0.97	5.581	7.617	4.974	4.582	4.552	5.454
0.98	6.908	9.280	5.764	5.239	5.219	6.391
0.99	9.274	12.890	7.563	6.695	6.680	8.041

Table 5 (Cont'd). Cumulative Distributions of Zenith Atmospheric Noise Temperature at
X-Band for Canberra DSCC, K

CD	July	August	September	October	November	December	Minimum	Year Average	Maximum
0.00	2.280	2.280	2.280	2.280	2.280	2.280	2.280	2.280	2.280
0.10	2.466	2.460	2.491	2.502	2.592	2.583	2.460	2.509	2.764
0.20	2.525	2.516	2.562	2.580	2.682	2.692	2.516	2.589	2.899
0.25	2.552	2.541	2.593	2.613	2.725	2.739	2.541	2.628	2.960
0.30	2.577	2.566	2.624	2.646	2.768	2.785	2.566	2.666	3.023
0.40	2.627	2.618	2.682	2.709	2.856	2.878	2.618	2.747	3.136
0.50	2.684	2.669	2.746	2.776	2.948	2.979	2.669	2.836	3.250
0.60	2.753	2.726	2.817	2.847	3.065	3.094	2.726	2.943	3.372
0.70	2.839	2.802	2.905	2.941	3.222	3.224	2.802	3.084	3.525
0.80	2.957	2.912	3.031	3.103	3.455	3.437	2.912	3.288	3.781
0.85	3.057	3.001	3.135	3.244	3.644	3.604	3.001	3.447	4.006
0.90	3.258	3.173	3.340	3.502	4.036	3.914	3.173	3.704	4.335
0.92	3.398	3.319	3.514	3.688	4.346	4.130	3.319	3.883	4.594
0.93	3.508	3.433	3.639	3.832	4.597	4.274	3.433	4.006	4.818
0.94	3.651	3.576	3.795	4.016	4.897	4.491	3.576	4.171	5.193
0.95	3.847	3.786	4.024	4.266	5.281	4.834	3.786	4.397	5.718
0.96	4.125	4.105	4.395	4.630	5.926	5.328	4.105	4.751	6.504
0.97	4.517	4.640	4.968	5.149	6.873	6.194	4.517	5.352	7.617
0.98	5.255	5.590	5.778	6.053	8.225	7.560	5.219	6.392	9.280
0.99	6.614	7.298	7.886	8.183	10.667	10.197	6.614	8.525	12.890

Table 6. Cumulative Distributions of Zenith Atmospheric Noise Temperature at X-Band
for Madrid DSCC, K

CD	January	February	March	April	May	June
0.00	2.239	2.239	2.239	2.239	2.239	2.239
0.10	2.319	2.333	2.375	2.416	2.496	2.527
0.20	2.389	2.399	2.448	2.489	2.579	2.622
0.25	2.422	2.431	2.481	2.522	2.616	2.664
0.30	2.455	2.462	2.516	2.555	2.654	2.703
0.40	2.520	2.520	2.582	2.622	2.731	2.778
0.50	2.592	2.585	2.648	2.700	2.806	2.849
0.60	2.682	2.664	2.720	2.777	2.887	2.926
0.70	2.815	2.774	2.818	2.854	2.984	3.017
0.80	3.016	2.971	2.997	3.003	3.127	3.115
0.85	3.217	3.179	3.187	3.183	3.272	3.173
0.90	3.703	3.752	3.662	3.647	3.672	3.254
0.92	4.108	4.249	4.043	3.998	4.013	3.313
0.93	4.410	4.577	4.311	4.255	4.256	3.354
0.94	4.820	4.962	4.645	4.598	4.568	3.419
0.95	5.308	5.439	5.091	5.046	4.975	3.527
0.96	5.909	6.013	5.653	5.584	5.536	3.675
0.97	6.649	6.699	6.446	6.317	6.240	3.976
0.98	7.590	7.780	7.491	7.347	7.338	4.681
0.99	9.146	10.602	9.179	8.980	9.593	6.459

Table 6 (Cont'd). Cumulative Distributions of Zenith Atmospheric Noise Temperature at
X-Band for Madrid DSCC, K

CD	July	August	September	October	November	December	Minimum	Year Average	Maximum
0.00	2.239	2.239	2.239	2.239	2.239	2.239	2.239	2.239	2.239
0.10	2.555	2.559	2.520	2.483	2.373	2.355	2.319	2.404	2.559
0.20	2.636	2.650	2.613	2.590	2.448	2.430	2.389	2.499	2.650
0.25	2.668	2.688	2.651	2.632	2.482	2.461	2.422	2.542	2.688
0.30	2.700	2.723	2.688	2.672	2.515	2.492	2.455	2.584	2.723
0.40	2.763	2.791	2.772	2.753	2.579	2.555	2.520	2.668	2.791
0.50	2.825	2.855	2.849	2.854	2.653	2.637	2.585	2.754	2.855
0.60	2.891	2.923	2.927	2.965	2.754	2.738	2.664	2.847	2.965
0.70	2.963	3.001	3.012	3.105	2.885	2.877	2.774	2.955	3.105
0.80	3.048	3.087	3.126	3.412	3.104	3.132	2.971	3.098	3.412
0.85	3.098	3.138	3.204	3.802	3.331	3.362	3.098	3.208	3.802
0.90	3.158	3.202	3.319	4.670	3.989	3.877	3.158	3.485	4.670
0.92	3.190	3.237	3.415	5.314	4.586	4.278	3.190	3.764	5.314
0.93	3.212	3.259	3.478	5.740	4.997	4.579	3.212	3.981	5.740
0.94	3.238	3.286	3.567	6.280	5.461	4.981	3.238	4.284	6.280
0.95	3.267	3.324	3.702	6.881	5.960	5.504	3.267	4.705	6.881
0.96	3.300	3.379	3.906	7.658	6.593	6.119	3.300	5.299	7.658
0.97	3.343	3.482	4.276	8.690	7.358	6.912	3.343	6.085	8.690
0.98	3.434	3.707	5.124	10.325	8.417	8.044	3.434	7.204	10.325
0.99	3.786	4.536	7.075	13.284	10.386	10.052	3.786	9.220	13.284

Table 7. Cumulative Distributions of Zenith Atmospheric Noise Temperature at Ka-Band
for Goldstone DSCC, K

CD	January	February	March	April	May	June
0.00	6.693	6.693	6.693	6.693	6.693	6.693
0.10	7.387	7.489	7.710	7.864	8.286	8.180
0.20	7.940	7.959	8.152	8.332	8.795	8.831
0.25	8.158	8.157	8.350	8.546	9.034	9.103
0.30	8.366	8.378	8.550	8.756	9.257	9.368
0.40	8.769	8.826	8.946	9.151	9.697	9.909
0.50	9.183	9.228	9.314	9.502	10.132	10.564
0.60	9.680	9.690	9.684	9.910	10.659	11.257
0.70	10.248	10.309	10.137	10.390	11.357	12.253
0.80	11.251	11.317	10.811	10.974	12.351	13.643
0.85	12.154	12.175	11.320	11.397	13.040	14.401
0.90	13.558	13.781	12.072	11.965	14.022	15.282
0.92	14.545	15.132	12.572	12.314	14.560	15.786
0.93	15.381	16.440	12.981	12.523	14.928	16.142
0.94	16.604	18.169	13.392	12.790	15.523	16.550
0.95	18.421	20.574	13.960	13.217	16.311	17.036
0.96	21.328	24.083	15.151	13.857	17.522	17.947
0.97	25.367	28.690	17.474	15.062	19.256	19.135
0.98	32.106	36.676	21.430	17.761	24.107	22.473
0.99	47.790	51.483	32.661	26.277	32.206	31.250

Table 7 (Cont'd). Cumulative Distributions of Zenith Atmospheric Noise Temperature at
Ka-Band for Goldstone DSCC, K

CD	July	August	September	October	November	December	Minimum	Year Average	Maximum
0.00	6.693	6.693	6.693	6.693	6.693	6.693	6.693	6.693	6.693
0.10	8.872	8.905	8.540	8.221	7.713	7.503	7.387	7.919	8.905
0.20	9.954	9.833	9.164	8.935	8.218	8.013	7.940	8.520	9.954
0.25	10.445	10.241	9.417	9.194	8.443	8.241	8.157	8.789	10.445
0.30	10.877	10.660	9.668	9.428	8.686	8.454	8.366	9.045	10.877
0.40	11.704	11.705	10.211	9.883	9.181	8.847	8.769	9.545	11.705
0.50	12.941	12.893	10.926	10.371	9.710	9.246	9.183	10.090	12.941
0.60	14.640	14.075	11.892	10.906	10.285	9.715	9.680	10.771	14.640
0.70	16.132	15.403	13.096	11.566	11.032	10.446	10.137	11.695	16.132
0.80	17.449	16.749	14.983	12.545	12.051	11.466	10.811	13.220	17.449
0.85	18.243	17.743	16.142	13.131	12.853	12.269	11.320	14.425	18.243
0.90	19.189	19.068	17.405	14.141	13.995	13.473	11.965	16.141	19.189
0.92	19.694	19.621	18.074	14.788	14.716	14.180	12.314	16.989	19.694
0.93	20.082	19.969	18.409	15.208	15.262	14.664	12.523	17.519	20.082
0.94	20.565	20.416	18.780	15.660	15.779	15.456	12.790	18.151	20.565
0.95	21.194	20.903	19.228	16.207	16.306	16.783	13.217	18.867	21.194
0.96	22.097	21.567	19.817	16.983	16.972	18.958	13.857	19.763	24.083
0.97	23.468	22.566	20.679	18.192	18.785	22.478	15.062	21.372	28.690
0.98	26.565	25.128	22.790	20.924	23.183	28.431	17.761	25.260	36.676
0.99	34.857	28.622	30.030	29.984	34.996	46.045	26.277	35.311	51.483

Table 8. Cumulative Distributions of Zenith Atmospheric Noise Temperature at Ka-Band
for Canberra DSCC, K

CD	January	February	March	April	May	June
0.00	7.173	7.173	7.173	7.173	7.173	7.173
0.10	11.932	13.702	12.103	10.806	10.396	9.720
0.20	13.379	15.336	13.382	11.911	11.104	10.290
0.25	13.982	16.057	13.874	12.326	11.398	10.559
0.30	14.559	16.792	14.377	12.666	11.677	10.812
0.40	15.737	18.113	15.383	13.329	12.210	11.408
0.50	16.946	19.422	16.616	14.093	12.748	12.116
0.60	18.347	20.852	17.995	15.125	13.339	13.105
0.70	20.233	22.675	19.571	16.273	14.200	14.386
0.80	22.953	25.872	21.783	17.734	15.807	16.130
0.85	24.876	28.734	23.384	18.818	17.227	17.525
0.90	27.860	32.908	26.109	20.880	20.040	20.608
0.92	30.141	36.204	27.619	22.419	22.231	23.232
0.93	31.676	39.029	28.526	23.518	23.714	25.054
0.94	33.554	43.699	29.867	25.184	25.461	27.771
0.95	36.251	50.110	32.005	27.665	27.765	32.256
0.96	40.158	59.425	35.457	31.358	30.918	38.704
0.97	48.413	72.023	40.908	35.950	35.556	46.862
0.98	64.059	89.600	50.625	44.197	43.945	58.075
0.99	89.543	123.144	71.405	61.596	61.418	76.624

Table 8 (Cont'd). Cumulative Distributions of Zenith Atmospheric Noise Temperature at
Ka-Band for Canberra DSCC, K

CD	July	August	September	October	November	December	Minimum	Year Average	Maximum
0.00	7.173	7.173	7.173	7.173	7.173	7.173	7.173	7.173	7.173
0.10	9.555	9.472	9.906	10.060	11.313	11.195	9.472	10.154	13.702
0.20	10.145	10.017	10.657	10.909	12.326	12.471	10.017	11.041	15.336
0.25	10.397	10.244	10.967	11.253	12.810	13.004	10.244	11.458	16.057
0.30	10.629	10.478	11.277	11.596	13.281	13.518	10.478	11.876	16.792
0.40	11.081	10.952	11.858	12.231	14.262	14.574	10.952	12.761	18.113
0.50	11.645	11.422	12.497	12.913	15.301	15.726	11.422	13.758	19.422
0.60	12.357	11.988	13.247	13.671	16.672	17.071	11.988	14.997	20.852
0.70	13.321	12.794	14.232	14.733	18.582	18.608	12.794	16.695	22.675
0.80	14.712	14.084	15.728	16.716	21.507	21.263	14.084	19.246	25.872
0.85	15.978	15.200	17.040	18.539	23.932	23.397	15.200	21.286	28.734
0.90	18.603	17.451	19.727	21.919	29.017	27.403	17.451	24.618	32.908
0.92	20.460	19.389	22.033	24.364	33.008	30.198	19.389	26.958	36.204
0.93	21.930	20.920	23.686	26.255	36.212	32.052	20.920	28.559	39.029
0.94	23.828	22.814	25.744	28.663	40.003	34.837	22.814	30.702	43.699
0.95	26.411	25.598	28.746	31.913	44.777	39.182	25.598	33.611	50.110
0.96	30.047	29.793	33.562	36.578	52.598	45.334	29.793	38.111	59.425
0.97	35.105	36.687	40.838	43.102	63.667	55.774	35.105	45.608	72.023
0.98	44.401	48.510	50.787	54.088	78.616	71.380	43.945	58.090	89.600
0.99	60.655	68.451	74.946	78.153	103.207	98.705	60.655	81.790	123.144

Table 9. Cumulative Distributions of Zenith Atmospheric Noise Temperature at Ka-Band
for Madrid DSCC, K

CD	January	February	March	April	May	June
0.00	7.031	7.031	7.031	7.031	7.031	7.031
0.10	7.917	8.116	8.715	9.288	10.414	10.847
0.20	8.667	8.815	9.499	10.079	11.329	11.929
0.25	9.014	9.135	9.848	10.416	11.734	12.397
0.30	9.355	9.452	10.212	10.754	12.137	12.817
0.40	10.035	10.036	10.897	11.465	12.977	13.632
0.50	10.800	10.710	11.589	12.306	13.777	14.377
0.60	11.826	11.574	12.346	13.138	14.669	15.209
0.70	13.442	12.868	13.480	13.984	15.770	16.223
0.80	15.982	15.364	15.723	15.801	17.506	17.338
0.85	18.624	18.101	18.211	18.157	19.366	18.012
0.90	25.049	25.707	24.508	24.309	24.641	19.004
0.92	30.357	32.191	29.500	28.914	29.105	19.764
0.93	34.240	36.391	32.975	32.238	32.260	20.299
0.94	39.448	41.239	37.239	36.641	36.253	21.150
0.95	45.521	47.130	42.834	42.262	41.378	22.593
0.96	52.798	54.035	49.709	48.880	48.292	24.545
0.97	61.472	62.056	59.116	57.616	56.709	28.512
0.98	72.073	74.162	70.976	69.380	69.279	37.615
0.99	88.574	102.902	88.910	86.871	93.083	59.247

Table 9 (Cont'd). Cumulative Distributions of Zenith Atmospheric Noise Temperature at
Ka-Band for Madrid DSCC, K

CD	July	August	September	October	November	December	Minimum	Year Average	Maximum
0.00	7.031	7.031	7.031	7.031	7.031	7.031	7.031	7.031	7.031
0.10	11.231	11.291	10.753	10.232	8.679	8.434	7.917	9.118	11.291
0.20	12.130	12.323	11.812	11.481	9.498	9.242	8.667	10.210	12.323
0.25	12.459	12.734	12.215	11.954	9.857	9.567	9.014	10.692	12.734
0.30	12.785	13.106	12.618	12.387	10.203	9.877	9.355	11.160	13.106
0.40	13.417	13.810	13.548	13.277	10.855	10.526	10.035	12.100	13.810
0.50	14.046	14.458	14.379	14.448	11.660	11.431	10.710	13.065	14.458
0.60	14.722	15.164	15.217	15.740	12.820	12.605	11.574	14.108	15.740
0.70	15.481	16.003	16.162	17.427	14.406	14.289	12.868	15.370	17.427
0.80	16.425	16.954	17.493	21.368	17.194	17.564	15.364	17.106	21.368
0.85	16.990	17.541	18.439	26.471	20.164	20.586	16.990	18.494	26.471
0.90	17.697	18.301	19.889	37.624	28.836	27.355	17.697	22.131	37.624
0.92	18.085	18.734	21.140	45.639	36.525	32.560	18.085	25.817	45.639
0.93	18.363	19.004	21.973	50.818	41.688	36.413	18.363	28.671	50.818
0.94	18.693	19.349	23.146	57.229	47.408	41.475	18.693	32.601	57.229
0.95	19.067	19.849	24.932	64.158	53.424	47.924	19.067	37.982	64.158
0.96	19.493	20.572	27.620	72.847	60.846	55.300	19.493	45.384	72.847
0.97	20.056	21.932	32.427	83.872	69.514	64.492	20.056	54.876	83.872
0.98	21.266	24.932	43.186	100.258	81.000	77.019	21.266	67.778	100.258
0.99	25.961	35.742	66.313	126.721	100.838	97.609	25.961	89.323	126.721

Table 10. Cumulative Distributions of Zenith Atmospheric Attenuation at
L- and S-Bands for Goldstone DSCC, dB

CD	January	February	March	April	May	June
0.00	0.033	0.033	0.033	0.033	0.033	0.033
0.10	0.033	0.033	0.033	0.033	0.033	0.033
0.20	0.033	0.033	0.033	0.033	0.033	0.033
0.25	0.033	0.033	0.033	0.033	0.033	0.033
0.30	0.033	0.033	0.033	0.033	0.034	0.034
0.40	0.033	0.033	0.033	0.033	0.034	0.034
0.50	0.033	0.033	0.033	0.034	0.034	0.034
0.60	0.034	0.034	0.034	0.034	0.034	0.034
0.70	0.034	0.034	0.034	0.034	0.034	0.034
0.80	0.034	0.034	0.034	0.034	0.034	0.034
0.85	0.034	0.034	0.034	0.034	0.034	0.034
0.90	0.034	0.034	0.034	0.034	0.034	0.034
0.92	0.034	0.034	0.034	0.034	0.034	0.034
0.93	0.034	0.034	0.034	0.034	0.034	0.034
0.94	0.034	0.034	0.034	0.034	0.034	0.034
0.95	0.034	0.034	0.034	0.034	0.034	0.034
0.96	0.034	0.035	0.034	0.034	0.034	0.034
0.97	0.035	0.035	0.034	0.034	0.034	0.034
0.98	0.035	0.036	0.034	0.034	0.035	0.035
0.99	0.037	0.037	0.035	0.035	0.035	0.035

Table 10 (Cont'd). Cumulative Distributions of Zenith Atmospheric Attenuation at
L- and S-Bands for Goldstone DSCC, dB

CD	July	August	September	October	November	December	Minimum	Year Average	Maximum
0.00	0.033	0.033	0.033	0.033	0.033	0.033	0.033	0.033	0.033
0.10	0.033	0.033	0.033	0.033	0.033	0.033	0.033	0.033	0.033
0.20	0.034	0.034	0.034	0.033	0.033	0.033	0.033	0.033	0.034
0.25	0.034	0.034	0.034	0.034	0.033	0.033	0.033	0.033	0.034
0.30	0.034	0.034	0.034	0.034	0.033	0.033	0.033	0.033	0.034
0.40	0.034	0.034	0.034	0.034	0.033	0.033	0.033	0.034	0.034
0.50	0.034	0.034	0.034	0.034	0.034	0.033	0.033	0.034	0.034
0.60	0.034	0.034	0.034	0.034	0.034	0.034	0.034	0.034	0.034
0.70	0.034	0.034	0.034	0.034	0.034	0.034	0.034	0.034	0.034
0.80	0.034	0.034	0.034	0.034	0.034	0.034	0.034	0.034	0.034
0.85	0.034	0.034	0.034	0.034	0.034	0.034	0.034	0.034	0.034
0.90	0.034	0.034	0.034	0.034	0.034	0.034	0.034	0.034	0.034
0.92	0.034	0.034	0.034	0.034	0.034	0.034	0.034	0.034	0.034
0.93	0.034	0.034	0.034	0.034	0.034	0.034	0.034	0.034	0.034
0.94	0.034	0.034	0.034	0.034	0.034	0.034	0.034	0.034	0.034
0.95	0.034	0.034	0.034	0.034	0.034	0.034	0.034	0.034	0.034
0.96	0.035	0.035	0.034	0.034	0.034	0.034	0.034	0.034	0.035
0.97	0.035	0.035	0.034	0.034	0.034	0.035	0.034	0.034	0.035
0.98	0.035	0.035	0.035	0.034	0.035	0.035	0.034	0.035	0.036
0.99	0.036	0.035	0.035	0.035	0.036	0.037	0.035	0.036	0.037

Table 11. Cumulative Distributions of Zenith Atmospheric Attenuation at
L- and S-Bands for Canberra DSCC, dB

CD	January	February	March	April	May	June
0.00	0.036	0.036	0.036	0.036	0.036	0.036
0.10	0.036	0.036	0.036	0.036	0.036	0.036
0.20	0.036	0.036	0.036	0.036	0.036	0.036
0.25	0.036	0.036	0.036	0.036	0.036	0.036
0.30	0.036	0.036	0.036	0.036	0.036	0.036
0.40	0.036	0.036	0.036	0.036	0.036	0.036
0.50	0.036	0.037	0.036	0.036	0.036	0.036
0.60	0.036	0.037	0.036	0.036	0.036	0.036
0.70	0.037	0.037	0.037	0.036	0.036	0.036
0.80	0.037	0.037	0.037	0.036	0.036	0.036
0.85	0.037	0.037	0.037	0.036	0.036	0.036
0.90	0.037	0.038	0.037	0.037	0.037	0.037
0.92	0.037	0.038	0.037	0.037	0.037	0.037
0.93	0.038	0.038	0.037	0.037	0.037	0.037
0.94	0.038	0.039	0.037	0.037	0.037	0.037
0.95	0.038	0.039	0.038	0.037	0.037	0.038
0.96	0.038	0.040	0.038	0.038	0.037	0.038
0.97	0.039	0.042	0.038	0.038	0.038	0.039
0.98	0.041	0.043	0.039	0.039	0.039	0.040
0.99	0.043	0.048	0.041	0.040	0.040	0.042

Table 11 (Cont'd). Cumulative Distributions of Zenith Atmospheric Attenuation at
L- and S-Bands for Canberra DSCC, dB

CD	July	August	September	October	November	December	Minimum	Year Average	Maximum
0.00	0.036	0.036	0.036	0.036	0.036	0.036	0.036	0.036	0.036
0.10	0.036	0.036	0.036	0.036	0.036	0.036	0.036	0.036	0.036
0.20	0.036	0.036	0.036	0.036	0.036	0.036	0.036	0.036	0.036
0.25	0.036	0.036	0.036	0.036	0.036	0.036	0.036	0.036	0.036
0.30	0.036	0.036	0.036	0.036	0.036	0.036	0.036	0.036	0.036
0.40	0.036	0.036	0.036	0.036	0.036	0.036	0.036	0.036	0.036
0.50	0.036	0.036	0.036	0.036	0.036	0.036	0.036	0.036	0.037
0.60	0.036	0.036	0.036	0.036	0.036	0.036	0.036	0.036	0.037
0.70	0.036	0.036	0.036	0.036	0.036	0.036	0.036	0.036	0.037
0.80	0.036	0.036	0.036	0.036	0.037	0.037	0.036	0.036	0.037
0.85	0.036	0.036	0.036	0.036	0.037	0.037	0.036	0.037	0.037
0.90	0.036	0.036	0.037	0.037	0.037	0.037	0.036	0.037	0.038
0.92	0.037	0.036	0.037	0.037	0.038	0.037	0.036	0.037	0.038
0.93	0.037	0.037	0.037	0.037	0.038	0.038	0.037	0.037	0.038
0.94	0.037	0.037	0.037	0.037	0.038	0.038	0.037	0.037	0.039
0.95	0.037	0.037	0.037	0.038	0.039	0.038	0.037	0.038	0.039
0.96	0.037	0.037	0.038	0.038	0.040	0.039	0.037	0.038	0.040
0.97	0.038	0.038	0.038	0.039	0.041	0.040	0.038	0.039	0.042
0.98	0.039	0.039	0.039	0.040	0.042	0.041	0.039	0.040	0.043
0.99	0.040	0.041	0.042	0.042	0.045	0.045	0.040	0.043	0.048

Table 12. Cumulative Distributions of Zenith Atmospheric Attenuation at
L- and S-Bands for Madrid DSCC, dB

CD	January	February	March	April	May	June
0.00	0.035	0.035	0.035	0.035	0.035	0.035
0.10	0.035	0.035	0.035	0.035	0.035	0.035
0.20	0.035	0.035	0.035	0.035	0.035	0.035
0.25	0.035	0.035	0.035	0.035	0.035	0.035
0.30	0.035	0.035	0.035	0.035	0.035	0.035
0.40	0.035	0.035	0.035	0.035	0.035	0.035
0.50	0.035	0.035	0.035	0.035	0.035	0.035
0.60	0.035	0.035	0.035	0.035	0.035	0.035
0.70	0.035	0.035	0.035	0.035	0.036	0.036
0.80	0.036	0.035	0.035	0.035	0.036	0.036
0.85	0.036	0.036	0.036	0.036	0.036	0.036
0.90	0.036	0.036	0.036	0.036	0.036	0.036
0.92	0.037	0.037	0.037	0.037	0.037	0.036
0.93	0.037	0.037	0.037	0.037	0.037	0.036
0.94	0.038	0.038	0.037	0.037	0.037	0.036
0.95	0.038	0.038	0.038	0.038	0.038	0.036
0.96	0.039	0.039	0.039	0.038	0.038	0.036
0.97	0.040	0.040	0.039	0.039	0.039	0.037
0.98	0.041	0.041	0.041	0.041	0.041	0.037
0.99	0.043	0.044	0.043	0.042	0.043	0.039

Table 12 (Cont'd). Cumulative Distributions of Zenith Atmospheric Attenuation at
L- and S-Bands for Madrid DSCC, dB

CD	July	August	September	October	November	December	Minimum	Year Average	Maximum
0.00	0.035	0.035	0.035	0.035	0.035	0.035	0.035	0.035	0.035
0.10	0.035	0.035	0.035	0.035	0.035	0.035	0.035	0.035	0.035
0.20	0.035	0.035	0.035	0.035	0.035	0.035	0.035	0.035	0.035
0.25	0.035	0.035	0.035	0.035	0.035	0.035	0.035	0.035	0.035
0.30	0.035	0.035	0.035	0.035	0.035	0.035	0.035	0.035	0.035
0.40	0.035	0.035	0.035	0.035	0.035	0.035	0.035	0.035	0.035
0.50	0.035	0.035	0.035	0.035	0.035	0.035	0.035	0.035	0.035
0.60	0.035	0.035	0.035	0.036	0.035	0.035	0.035	0.035	0.036
0.70	0.035	0.036	0.036	0.036	0.035	0.035	0.035	0.035	0.036
0.80	0.036	0.036	0.036	0.036	0.036	0.036	0.035	0.036	0.036
0.85	0.036	0.036	0.036	0.036	0.036	0.036	0.035	0.036	0.036
0.90	0.036	0.036	0.036	0.037	0.037	0.037	0.036	0.036	0.037
0.92	0.036	0.036	0.036	0.038	0.037	0.038	0.036	0.037	0.038
0.93	0.036	0.036	0.036	0.039	0.038	0.038	0.036	0.037	0.039
0.94	0.036	0.036	0.036	0.039	0.038	0.039	0.036	0.037	0.039
0.95	0.036	0.036	0.036	0.040	0.039	0.039	0.036	0.038	0.040
0.96	0.036	0.036	0.037	0.041	0.039	0.040	0.036	0.038	0.041
0.97	0.036	0.036	0.037	0.042	0.040	0.041	0.036	0.039	0.042
0.98	0.036	0.036	0.038	0.044	0.041	0.042	0.036	0.040	0.044
0.99	0.036	0.037	0.041	0.047	0.044	0.045	0.036	0.042	0.047

Table 13. Cumulative Distributions of Zenith Atmospheric Attenuation at X-Band
for Goldstone DSCC, dB

CD	January	February	March	April	May	June
0.00	0.037	0.037	0.037	0.037	0.037	0.037
0.10	0.037	0.037	0.038	0.038	0.038	0.038
0.20	0.038	0.038	0.038	0.038	0.039	0.039
0.25	0.038	0.038	0.038	0.039	0.039	0.039
0.30	0.038	0.038	0.039	0.039	0.039	0.040
0.40	0.039	0.039	0.039	0.039	0.040	0.040
0.50	0.039	0.039	0.039	0.039	0.040	0.041
0.60	0.040	0.040	0.040	0.040	0.041	0.041
0.70	0.040	0.040	0.040	0.040	0.041	0.042
0.80	0.041	0.041	0.041	0.041	0.042	0.044
0.85	0.042	0.042	0.041	0.041	0.043	0.045
0.90	0.044	0.044	0.042	0.042	0.044	0.046
0.92	0.045	0.045	0.043	0.042	0.045	0.046
0.93	0.046	0.047	0.043	0.042	0.045	0.047
0.94	0.047	0.049	0.043	0.043	0.046	0.047
0.95	0.049	0.052	0.044	0.043	0.047	0.048
0.96	0.053	0.056	0.045	0.044	0.048	0.049
0.97	0.057	0.061	0.048	0.045	0.050	0.050
0.98	0.065	0.071	0.053	0.048	0.056	0.054
0.99	0.085	0.090	0.066	0.058	0.065	0.064

Table 13 (Cont'd). Cumulative Distributions of Zenith Atmospheric Attenuation at X-Band
for Goldstone DSCC, dB

CD	July	August	September	October	November	December	Minimum	Year Average	Maximum
0.00	0.037	0.037	0.037	0.037	0.037	0.037	0.037	0.037	0.037
0.10	0.039	0.039	0.039	0.038	0.038	0.037	0.037	0.038	0.039
0.20	0.040	0.040	0.039	0.039	0.038	0.038	0.038	0.039	0.040
0.25	0.041	0.041	0.040	0.039	0.038	0.038	0.038	0.039	0.041
0.30	0.041	0.041	0.040	0.040	0.039	0.038	0.038	0.039	0.041
0.40	0.042	0.042	0.040	0.040	0.039	0.039	0.039	0.040	0.042
0.50	0.044	0.043	0.041	0.040	0.040	0.039	0.039	0.040	0.044
0.60	0.045	0.045	0.042	0.041	0.040	0.040	0.040	0.041	0.045
0.70	0.047	0.046	0.043	0.042	0.041	0.040	0.040	0.042	0.047
0.80	0.048	0.047	0.045	0.043	0.042	0.041	0.041	0.043	0.048
0.85	0.049	0.049	0.047	0.043	0.043	0.042	0.041	0.045	0.049
0.90	0.050	0.050	0.048	0.044	0.044	0.044	0.042	0.047	0.050
0.92	0.051	0.051	0.049	0.045	0.045	0.044	0.042	0.048	0.051
0.93	0.051	0.051	0.049	0.046	0.046	0.045	0.042	0.048	0.051
0.94	0.052	0.051	0.050	0.046	0.046	0.046	0.043	0.049	0.052
0.95	0.052	0.052	0.050	0.047	0.047	0.047	0.043	0.050	0.052
0.96	0.053	0.053	0.051	0.047	0.047	0.050	0.044	0.051	0.056
0.97	0.055	0.054	0.052	0.049	0.050	0.054	0.045	0.053	0.061
0.98	0.059	0.057	0.054	0.052	0.055	0.061	0.048	0.057	0.071
0.99	0.069	0.061	0.063	0.063	0.069	0.083	0.058	0.069	0.090

Table 14. Cumulative Distributions of Zenith Atmospheric Attenuation at X-Band
for Canberra DSCC, dB

CD	January	February	March	April	May	June
0.00	0.039	0.039	0.039	0.039	0.039	0.039
0.10	0.045	0.047	0.045	0.043	0.043	0.042
0.20	0.046	0.049	0.046	0.045	0.044	0.043
0.25	0.047	0.049	0.047	0.045	0.044	0.043
0.30	0.048	0.050	0.047	0.045	0.044	0.043
0.40	0.049	0.052	0.048	0.046	0.045	0.044
0.50	0.050	0.053	0.050	0.047	0.045	0.044
0.60	0.052	0.055	0.051	0.048	0.046	0.045
0.70	0.054	0.057	0.053	0.049	0.047	0.047
0.80	0.057	0.060	0.055	0.050	0.048	0.049
0.85	0.059	0.063	0.057	0.052	0.050	0.050
0.90	0.062	0.068	0.060	0.054	0.053	0.054
0.92	0.065	0.072	0.062	0.056	0.055	0.057
0.93	0.067	0.076	0.063	0.057	0.057	0.059
0.94	0.069	0.082	0.065	0.059	0.059	0.062
0.95	0.072	0.090	0.067	0.062	0.062	0.067
0.96	0.077	0.102	0.071	0.066	0.066	0.075
0.97	0.088	0.120	0.078	0.072	0.071	0.086
0.98	0.109	0.147	0.091	0.082	0.082	0.100
0.99	0.146	0.205	0.119	0.105	0.105	0.127

Table 14 (Cont'd). Cumulative Distributions of Zenith Atmospheric Attenuation at X-Band
for Canberra DSCC, dB

CD	July	August	September	October	November	December	Minimum	Year Average	Maximum
0.00	0.039	0.039	0.039	0.039	0.039	0.039	0.039	0.039	0.039
0.10	0.042	0.042	0.042	0.042	0.044	0.044	0.042	0.043	0.047
0.20	0.042	0.042	0.043	0.043	0.045	0.045	0.042	0.043	0.049
0.25	0.043	0.042	0.043	0.044	0.046	0.046	0.042	0.044	0.049
0.30	0.043	0.043	0.044	0.044	0.046	0.046	0.043	0.044	0.050
0.40	0.043	0.043	0.044	0.045	0.047	0.047	0.043	0.045	0.052
0.50	0.044	0.044	0.045	0.045	0.048	0.049	0.044	0.046	0.053
0.60	0.045	0.044	0.046	0.046	0.050	0.050	0.044	0.048	0.055
0.70	0.045	0.045	0.047	0.047	0.052	0.052	0.045	0.049	0.057
0.80	0.047	0.046	0.048	0.049	0.055	0.055	0.046	0.052	0.060
0.85	0.048	0.047	0.050	0.051	0.058	0.057	0.047	0.055	0.063
0.90	0.051	0.050	0.053	0.055	0.064	0.062	0.050	0.058	0.068
0.92	0.053	0.052	0.055	0.058	0.068	0.065	0.052	0.061	0.072
0.93	0.055	0.054	0.057	0.060	0.072	0.067	0.054	0.063	0.076
0.94	0.057	0.056	0.060	0.063	0.077	0.071	0.056	0.066	0.082
0.95	0.060	0.059	0.063	0.067	0.083	0.076	0.059	0.069	0.090
0.96	0.065	0.064	0.069	0.073	0.093	0.084	0.064	0.075	0.102
0.97	0.071	0.073	0.078	0.081	0.108	0.097	0.071	0.084	0.120
0.98	0.082	0.088	0.091	0.095	0.130	0.119	0.082	0.100	0.147
0.99	0.104	0.115	0.124	0.129	0.169	0.161	0.104	0.134	0.205

Table 15. Cumulative Distributions of Zenith Atmospheric Attenuation at X-Band
for Madrid DSCC, dB

CD	January	February	March	April	May	June
0.00	0.038	0.038	0.038	0.038	0.038	0.038
0.10	0.039	0.040	0.040	0.041	0.042	0.043
0.20	0.040	0.040	0.041	0.042	0.043	0.044
0.25	0.040	0.041	0.041	0.042	0.044	0.045
0.30	0.041	0.041	0.042	0.042	0.044	0.045
0.40	0.042	0.042	0.043	0.043	0.045	0.046
0.50	0.042	0.042	0.043	0.044	0.046	0.047
0.60	0.043	0.043	0.044	0.045	0.047	0.047
0.70	0.045	0.044	0.045	0.046	0.048	0.048
0.80	0.048	0.047	0.048	0.048	0.050	0.049
0.85	0.051	0.050	0.050	0.050	0.052	0.050
0.90	0.058	0.059	0.058	0.057	0.058	0.051
0.92	0.065	0.067	0.064	0.063	0.063	0.052
0.93	0.069	0.072	0.068	0.067	0.067	0.053
0.94	0.076	0.078	0.073	0.072	0.072	0.054
0.95	0.084	0.086	0.080	0.079	0.078	0.055
0.96	0.093	0.095	0.089	0.088	0.087	0.058
0.97	0.105	0.105	0.101	0.099	0.098	0.062
0.98	0.120	0.123	0.118	0.116	0.116	0.073
0.99	0.144	0.168	0.145	0.142	0.152	0.101

Table 15 (Cont'd). Cumulative Distributions of Zenith Atmospheric Attenuation at X-Band
for Madrid DSCC, dB

CD	July	August	September	October	November	December	Minimum	Year Average	Maximum
0.00	0.038	0.038	0.038	0.038	0.038	0.038	0.038	0.038	0.038
0.10	0.043	0.043	0.043	0.042	0.040	0.040	0.039	0.041	0.043
0.20	0.044	0.044	0.044	0.043	0.041	0.041	0.040	0.042	0.044
0.25	0.045	0.045	0.044	0.044	0.041	0.041	0.040	0.042	0.045
0.30	0.045	0.045	0.045	0.044	0.042	0.041	0.041	0.043	0.045
0.40	0.046	0.046	0.046	0.045	0.042	0.042	0.042	0.044	0.046
0.50	0.046	0.047	0.047	0.047	0.043	0.043	0.042	0.045	0.047
0.60	0.047	0.047	0.047	0.048	0.045	0.044	0.043	0.046	0.048
0.70	0.047	0.048	0.048	0.050	0.046	0.046	0.044	0.047	0.050
0.80	0.048	0.049	0.050	0.054	0.049	0.050	0.047	0.049	0.054
0.85	0.049	0.050	0.051	0.060	0.053	0.053	0.049	0.051	0.060
0.90	0.050	0.050	0.052	0.074	0.063	0.061	0.050	0.055	0.074
0.92	0.050	0.051	0.054	0.084	0.072	0.067	0.050	0.059	0.084
0.93	0.050	0.051	0.055	0.091	0.079	0.072	0.050	0.063	0.091
0.94	0.051	0.052	0.056	0.099	0.086	0.078	0.051	0.067	0.099
0.95	0.051	0.052	0.058	0.109	0.094	0.087	0.051	0.074	0.109
0.96	0.052	0.053	0.061	0.121	0.104	0.096	0.052	0.083	0.121
0.97	0.052	0.054	0.067	0.137	0.116	0.109	0.052	0.096	0.137
0.98	0.054	0.058	0.080	0.163	0.133	0.127	0.054	0.113	0.163
0.99	0.059	0.071	0.111	0.211	0.164	0.159	0.059	0.146	0.211

Table 16. Cumulative Distributions of Zenith Atmospheric Attenuation at Ka-Band
for Goldstone DSCC, dB

CD	January	February	March	April	May	June
0.00	0.116	0.116	0.116	0.116	0.116	0.116
0.10	0.126	0.128	0.132	0.135	0.142	0.140
0.20	0.135	0.135	0.138	0.141	0.149	0.150
0.25	0.138	0.138	0.141	0.144	0.153	0.154
0.30	0.141	0.141	0.144	0.147	0.156	0.158
0.40	0.146	0.147	0.149	0.153	0.162	0.166
0.50	0.152	0.152	0.154	0.157	0.168	0.175
0.60	0.159	0.159	0.159	0.162	0.175	0.185
0.70	0.166	0.167	0.165	0.169	0.185	0.200
0.80	0.181	0.182	0.174	0.177	0.200	0.221
0.85	0.195	0.196	0.182	0.183	0.210	0.233
0.90	0.218	0.221	0.193	0.191	0.225	0.246
0.92	0.233	0.243	0.201	0.197	0.234	0.254
0.93	0.247	0.264	0.207	0.200	0.239	0.260
0.94	0.267	0.293	0.214	0.204	0.249	0.266
0.95	0.297	0.333	0.223	0.211	0.262	0.274
0.96	0.345	0.392	0.242	0.221	0.282	0.289
0.97	0.414	0.471	0.281	0.241	0.310	0.308
0.98	0.530	0.611	0.346	0.285	0.392	0.364
0.99	0.814	0.883	0.539	0.428	0.531	0.514

Table 16 (Cont'd). Cumulative Distributions of Zenith Atmospheric Attenuation at Ka-Band
for Goldstone DSCC, dB

CD	July	August	September	October	November	December	Minimum	Year Average	Maximum
0.00	0.116	0.116	0.116	0.116	0.116	0.116	0.116	0.116	0.116
0.10	0.152	0.153	0.146	0.141	0.132	0.128	0.126	0.136	0.153
0.20	0.170	0.167	0.156	0.152	0.139	0.136	0.135	0.145	0.170
0.25	0.177	0.174	0.159	0.156	0.143	0.139	0.138	0.149	0.177
0.30	0.184	0.180	0.163	0.159	0.146	0.142	0.141	0.152	0.184
0.40	0.196	0.196	0.171	0.165	0.153	0.147	0.146	0.159	0.196
0.50	0.215	0.215	0.181	0.172	0.161	0.153	0.152	0.167	0.215
0.60	0.242	0.233	0.196	0.179	0.169	0.159	0.159	0.177	0.242
0.70	0.265	0.253	0.214	0.188	0.179	0.170	0.165	0.191	0.265
0.80	0.285	0.273	0.243	0.203	0.195	0.185	0.174	0.214	0.285
0.85	0.297	0.288	0.261	0.212	0.207	0.197	0.182	0.233	0.297
0.90	0.311	0.309	0.281	0.227	0.225	0.216	0.191	0.260	0.311
0.92	0.319	0.318	0.292	0.237	0.236	0.227	0.197	0.274	0.319
0.93	0.325	0.323	0.297	0.244	0.245	0.235	0.200	0.282	0.325
0.94	0.333	0.331	0.303	0.251	0.253	0.248	0.204	0.293	0.333
0.95	0.343	0.339	0.310	0.260	0.262	0.270	0.211	0.304	0.343
0.96	0.358	0.349	0.320	0.273	0.273	0.306	0.221	0.319	0.392
0.97	0.381	0.366	0.334	0.293	0.302	0.364	0.241	0.346	0.471
0.98	0.434	0.409	0.369	0.338	0.376	0.466	0.285	0.411	0.611
0.99	0.578	0.469	0.493	0.492	0.580	0.781	0.428	0.586	0.883

Table 17. Cumulative Distributions of Zenith Atmospheric Attenuation at Ka-Band
for Canberra DSCC, dB

CD	January	February	March	April	May	June
0.00	0.124	0.124	0.124	0.124	0.124	0.124
0.10	0.206	0.237	0.209	0.186	0.179	0.167
0.20	0.229	0.264	0.229	0.204	0.190	0.175
0.25	0.239	0.275	0.237	0.210	0.194	0.179
0.30	0.248	0.287	0.245	0.215	0.198	0.183
0.40	0.266	0.307	0.260	0.224	0.205	0.191
0.50	0.284	0.327	0.279	0.235	0.212	0.201
0.60	0.306	0.349	0.300	0.250	0.220	0.216
0.70	0.335	0.377	0.324	0.267	0.232	0.236
0.80	0.379	0.429	0.358	0.290	0.257	0.263
0.85	0.410	0.477	0.384	0.306	0.280	0.285
0.90	0.459	0.548	0.429	0.340	0.326	0.335
0.92	0.498	0.606	0.454	0.365	0.362	0.379
0.93	0.525	0.656	0.470	0.384	0.387	0.410
0.94	0.558	0.741	0.493	0.412	0.416	0.456
0.95	0.605	0.861	0.530	0.454	0.456	0.534
0.96	0.675	1.040	0.590	0.518	0.510	0.649
0.97	0.827	1.295	0.688	0.599	0.591	0.798
0.98	1.131	1.679	0.868	0.748	0.743	1.012
0.99	1.675	2.520	1.280	1.080	1.077	1.390

Table 17 (Cont'd). Cumulative Distributions of Zenith Atmospheric Attenuation at Ka-Band
for Canberra DSCC, dB

CD	July	August	September	October	November	December	Minimum	Year Average	Maximum
0.00	0.124	0.124	0.124	0.124	0.124	0.124	0.124	0.124	0.124
0.10	0.164	0.163	0.170	0.173	0.195	0.193	0.163	0.175	0.237
0.20	0.173	0.171	0.182	0.186	0.211	0.213	0.171	0.188	0.264
0.25	0.176	0.174	0.186	0.191	0.218	0.222	0.174	0.195	0.275
0.30	0.180	0.177	0.191	0.196	0.225	0.230	0.177	0.201	0.287
0.40	0.186	0.183	0.199	0.205	0.240	0.246	0.183	0.214	0.307
0.50	0.193	0.190	0.208	0.215	0.256	0.263	0.190	0.229	0.327
0.60	0.203	0.197	0.218	0.226	0.277	0.284	0.197	0.248	0.349
0.70	0.218	0.209	0.233	0.241	0.307	0.307	0.209	0.275	0.377
0.80	0.239	0.228	0.256	0.272	0.354	0.349	0.228	0.315	0.429
0.85	0.259	0.246	0.277	0.302	0.394	0.384	0.246	0.348	0.477
0.90	0.301	0.282	0.320	0.357	0.480	0.452	0.282	0.403	0.548
0.92	0.332	0.314	0.359	0.398	0.549	0.499	0.314	0.443	0.606
0.93	0.357	0.339	0.386	0.430	0.606	0.532	0.339	0.470	0.656
0.94	0.388	0.371	0.421	0.472	0.673	0.580	0.371	0.507	0.741
0.95	0.432	0.418	0.473	0.528	0.760	0.658	0.418	0.558	0.861
0.96	0.495	0.490	0.557	0.610	0.907	0.770	0.490	0.638	1.040
0.97	0.583	0.612	0.687	0.728	1.124	0.968	0.583	0.774	1.295
0.98	0.751	0.828	0.871	0.934	1.434	1.281	0.743	1.012	1.679
0.99	1.061	1.219	1.354	1.423	1.999	1.890	1.061	1.502	2.520

Table 18. Cumulative Distributions of Zenith Atmospheric Attenuation at Ka-Band
for Madrid DSCC, dB

CD	January	February	March	April	May	June
0.00	0.121	0.121	0.121	0.121	0.121	0.121
0.10	0.136	0.139	0.150	0.160	0.179	0.187
0.20	0.147	0.150	0.162	0.172	0.193	0.204
0.25	0.153	0.155	0.167	0.177	0.200	0.211
0.30	0.158	0.159	0.172	0.182	0.206	0.217
0.40	0.168	0.168	0.182	0.192	0.218	0.229
0.50	0.179	0.177	0.192	0.205	0.230	0.240
0.60	0.195	0.190	0.203	0.217	0.243	0.252
0.70	0.220	0.210	0.220	0.229	0.259	0.267
0.80	0.260	0.250	0.256	0.257	0.286	0.283
0.85	0.303	0.294	0.296	0.295	0.316	0.293
0.90	0.411	0.422	0.402	0.398	0.404	0.308
0.92	0.502	0.534	0.487	0.477	0.480	0.320
0.93	0.570	0.609	0.548	0.535	0.535	0.329
0.94	0.663	0.696	0.623	0.613	0.606	0.343
0.95	0.774	0.804	0.725	0.714	0.698	0.367
0.96	0.911	0.935	0.852	0.837	0.825	0.400
0.97	1.080	1.091	1.033	1.004	0.986	0.468
0.98	1.295	1.339	1.272	1.239	1.237	0.628
0.99	1.653	1.992	1.661	1.615	1.757	1.034

Table 18 (Cont'd). Cumulative Distributions of Zenith Atmospheric Attenuation at Ka-Band
for Madrid DSCC, dB

CD	July	August	September	October	November	December	Minimum	Year Average	Maximum
0.00	0.121	0.121	0.121	0.121	0.121	0.121	0.121	0.121	0.121
0.10	0.194	0.195	0.185	0.176	0.149	0.145	0.136	0.157	0.195
0.20	0.207	0.211	0.202	0.196	0.162	0.157	0.147	0.174	0.211
0.25	0.212	0.217	0.208	0.203	0.167	0.162	0.153	0.181	0.217
0.30	0.217	0.222	0.214	0.210	0.172	0.167	0.158	0.189	0.222
0.40	0.226	0.232	0.228	0.223	0.182	0.176	0.168	0.203	0.232
0.50	0.234	0.241	0.240	0.241	0.194	0.190	0.177	0.217	0.241
0.60	0.244	0.251	0.252	0.261	0.211	0.208	0.190	0.233	0.261
0.70	0.254	0.263	0.266	0.287	0.236	0.234	0.210	0.252	0.287
0.80	0.267	0.276	0.285	0.351	0.280	0.287	0.250	0.279	0.351
0.85	0.276	0.285	0.300	0.437	0.329	0.336	0.276	0.301	0.437
0.90	0.286	0.296	0.323	0.633	0.477	0.451	0.286	0.361	0.633
0.92	0.292	0.303	0.343	0.779	0.612	0.541	0.292	0.423	0.779
0.93	0.297	0.307	0.357	0.876	0.705	0.609	0.297	0.472	0.876
0.94	0.302	0.313	0.377	0.999	0.810	0.700	0.302	0.541	0.999
0.95	0.308	0.321	0.407	1.136	0.924	0.819	0.308	0.636	1.136
0.96	0.315	0.333	0.453	1.314	1.068	0.959	0.315	0.771	1.314
0.97	0.324	0.355	0.536	1.551	1.243	1.140	0.324	0.950	1.551
0.98	0.344	0.406	0.729	1.929	1.486	1.400	0.344	1.206	1.929
0.99	0.423	0.594	1.175	2.620	1.941	1.864	0.423	1.670	2.620

Table 19. Cumulative Distributions of Year-Average Zenith Atmospheric Attenuation
and Noise Temperature at K-Band for Goldstone DSCC

CD	25.5 GHz		26.0 GHz		26.5 GHz		27.0 GHz	
	A_{zen}, dB	T_{zen}, K	A_{zen}, dB	T_{zen}, K	A_{zen}, dB	T_{zen}, K	A_{zen}, dB	T_{zen}, K
0.00	0.076	4.382	0.078	4.513	0.080	4.650	0.083	4.794
0.10	0.110	6.485	0.109	6.417	0.109	6.406	0.110	6.441
0.20	0.122	7.215	0.120	7.099	0.120	7.053	0.120	7.063
0.25	0.127	7.534	0.125	7.396	0.124	7.336	0.124	7.335
0.30	0.132	7.840	0.130	7.682	0.129	7.607	0.129	7.596
0.40	0.142	8.476	0.139	8.276	0.138	8.169	0.137	8.137
0.50	0.154	9.192	0.150	8.944	0.148	8.804	0.147	8.747
0.60	0.168	10.058	0.163	9.753	0.160	9.571	0.159	9.486
0.70	0.185	11.099	0.179	10.725	0.175	10.495	0.173	10.375
0.80	0.206	12.405	0.199	11.947	0.194	11.656	0.192	11.493
0.85	0.221	13.292	0.212	12.780	0.207	12.449	0.204	12.259
0.90	0.242	14.567	0.232	13.977	0.226	13.590	0.222	13.360
0.92	0.255	15.407	0.245	14.766	0.238	14.343	0.234	14.088
0.93	0.266	16.019	0.254	15.342	0.247	14.893	0.243	14.619
0.94	0.279	16.803	0.267	16.082	0.259	15.600	0.254	15.303
0.95	0.297	17.890	0.284	17.107	0.275	16.580	0.270	16.252
0.96	0.324	19.479	0.309	18.608	0.299	18.017	0.293	17.644
0.97	0.367	22.000	0.350	20.994	0.338	20.306	0.331	19.864
0.98	0.454	27.036	0.432	25.779	0.417	24.905	0.407	24.333
0.99	0.656	38.214	0.623	36.480	0.600	35.254	0.585	34.430

Table 20. Cumulative Distributions of Year-Average Zenith Atmospheric Attenuation and
NoiseTemperature at K-Band for Canberra DSCC

CD	25.5 GHz		26.0 GHz		26.5 GHz		27.0 GHz	
	A_{zen}, dB	T_{zen}, K	A_{zen}, dB	T_{zen}, K	A_{zen}, dB	T_{zen}, K	A_{zen}, dB	T_{zen}, K
0.00	0.081	4.698	0.083	4.838	0.086	4.985	0.088	5.140
0.10	0.155	9.190	0.151	8.995	0.150	8.896	0.150	8.872
0.20	0.173	10.316	0.169	10.052	0.166	9.904	0.166	9.845
0.25	0.181	10.788	0.176	10.496	0.173	10.327	0.172	10.253
0.30	0.188	11.239	0.183	10.919	0.180	10.729	0.178	10.641
0.40	0.203	12.146	0.197	11.769	0.193	11.539	0.191	11.422
0.50	0.219	13.145	0.212	12.707	0.207	12.432	0.205	12.284
0.60	0.239	14.370	0.230	13.858	0.225	13.530	0.222	13.344
0.70	0.265	15.966	0.255	15.361	0.249	14.965	0.245	14.731
0.80	0.306	18.412	0.293	17.670	0.285	17.173	0.280	16.868
0.85	0.340	20.455	0.325	19.602	0.316	19.025	0.310	18.664
0.90	0.406	24.298	0.387	23.251	0.375	22.532	0.367	22.070
0.92	0.457	27.241	0.436	26.056	0.421	25.234	0.412	24.699
0.93	0.493	29.322	0.470	28.042	0.455	27.151	0.444	26.567
0.94	0.542	32.073	0.516	30.675	0.499	29.695	0.488	29.049
0.95	0.573	33.834	0.548	32.443	0.530	31.479	0.519	30.854
0.96	0.654	38.219	0.632	37.027	0.618	36.259	0.610	35.827
0.97	0.749	43.310	0.731	42.333	0.720	41.775	0.716	41.552
0.98	0.903	51.276	0.890	50.634	0.886	50.405	0.888	50.504
0.99	1.214	66.608	1.213	66.572	1.221	66.932	1.236	67.606

Table 21. Cumulative Distributions of Year-Average Zenith Atmospheric Attenuation and Noise Temperature at K-Band for Madrid DSCC

CD	25.5 GHz		26.0 GHz		26.5 GHz		27.0 GHz	
	A_{zen}, dB	T_{zen}, K	A_{zen}, dB	T_{zen}, K	A_{zen}, dB	T_{zen}, K	A_{zen}, dB	T_{zen}, K
0.00	0.079	4.605	0.082	4.742	0.084	4.886	0.087	5.037
0.10	0.132	7.815	0.130	7.690	0.129	7.641	0.130	7.650
0.20	0.149	8.865	0.146	8.674	0.145	8.578	0.144	8.554
0.25	0.156	9.294	0.153	9.076	0.151	8.959	0.150	8.922
0.30	0.163	9.706	0.159	9.462	0.157	9.327	0.156	9.276
0.40	0.177	10.563	0.172	10.265	0.169	10.089	0.168	10.011
0.50	0.191	11.472	0.186	11.117	0.182	10.901	0.181	10.793
0.60	0.208	12.530	0.202	12.108	0.197	11.844	0.195	11.703
0.70	0.230	13.871	0.222	13.368	0.217	13.044	0.214	12.861
0.80	0.268	16.138	0.257	15.501	0.250	15.081	0.246	14.830
0.85	0.307	18.490	0.294	17.722	0.286	17.207	0.280	16.889
0.90	0.404	24.150	0.385	23.090	0.373	22.361	0.365	21.892
0.92	0.484	28.753	0.461	27.477	0.445	26.589	0.435	26.007
0.93	0.507	30.114	0.485	28.863	0.470	28.001	0.460	27.447
0.94	0.585	34.408	0.561	33.085	0.545	32.187	0.535	31.626
0.95	0.639	37.366	0.616	36.140	0.602	35.341	0.594	34.881
0.96	0.704	40.842	0.683	39.757	0.671	39.097	0.666	38.775
0.97	0.785	45.123	0.768	44.228	0.759	43.754	0.757	43.615
0.98	0.906	51.374	0.893	50.733	0.889	50.508	0.892	50.613
0.99	1.136	62.772	1.132	62.589	1.137	62.809	1.149	63.349

Table 22. Monthly and Year-Average Rainfall Amounts at the DSN Antenna Locations

Month	Goldstone		Canberra		Madrid	
	inches	mm	inches	mm	inches	mm
January	1.02	25.9	3.61	91.7	1.48	37.5
February	1.18	30.0	2.74	69.7	1.38	35.0
March	0.90	22.9	2.90	73.6	1.10	28.0
April	0.20	5.1	2.85	72.4	1.87	47.5
May	0.19	4.8	2.94	74.8	1.56	39.5
June	0.04	1.0	2.70	68.7	1.26	32.0
July	0.35	8.9	3.36	85.3	0.57	14.5
August	0.59	15.0	3.90	99.0	0.59	15.0
September	0.39	9.9	3.73	94.7	1.16	29.5
October	0.15	3.8	3.70	94.0	1.54	39.0
November	0.23	5.8	3.50	88.8	2.01	51.0
December	0.57	14.5	2.42	61.4	1.75	44.5
Year Average	5.81	147.6	38.67	982.1	16.26	413.0

Table 23. Parameters for X-Band Planetary Noise Calculation, plus X-Band, K-band, and
Ka-Band Noise Temperatures at Mean Minimum Distance from Earth

Planet	Diameter (km)		Mean Distance from Earth (10^6 km)		Mean Distance from Sun		Blackbody Disk Temp (K)	T_{planet} at Mean Minimum Distance (K)			
								X-Band		K-Band	Ka-Band
								70-m (74.4 dBi gain)	34-m (68.3 dBi gain)	34-m (77.2 dBi gain)	34-m (78.8 dBi gain)
	polar	equatorial	min.	max.	(10^6 km)	AU					
Mercury		4880	91.7	207.5	57.9	0.387	625	3.05	0.75	5.81	8.39
Venus		12104	41.4	257.8	108.2	0.723	634 (X-band) 497 (K-band) 472 (Ka-band)	93.29 – –	22.90 – –	– 139.35 –	– – 191.28
Earth		12757	–	–	149.6	1.000	250–300 [1]	–	–	–	–
Mars		6794	78.3	377.5	227.9	1.523	180	2.33	0.57	4.45	6.43
Jupiter	134102	142984	628.7	927.9	778.3	5.203	152	13.53	3.32	25.79	37.27
Saturn	108728	120536	1279.8	1579.0	1429.4	9.555	155	2.37	0.58	4.51	6.52
Uranus		51118	2721.4	3020.6	2871.0	19.191	160	0.10	0.02	0.19	0.27
Neptune		49532	4354.4	4653.6	4504.0	30.107	160	0.04	0.01	0.07	0.10
Pluto		2274	5763.9	6063.1	5913.5	39.529	160	0.00	0.00	0.00	0.00

Note:

1. Ocean (250 K) and Land (300 K)